REMARKS

Claims 1, 3, 4, 6-11, 13, 14, 16-21, 23, 24, 26-31, 33, 34, and 36- 42 are pending. Claims 2, 5, 12, 15, 22, 25, 32 and 35 are cancelled without prejudice as being redundant in view of amendments made to the claims. Claims 20, 30 and 40 are cancelled without prejudice to further prosecution in other applications. Claims 43-50 are cancelled without prejudice as being drawn to a non-elected invention. Claims 1, 11, 31, 36 and 42 and dependent claims 6, 8, 16, 18, 33, 19, 36 and 38 are currently amended to more clearly set forth the subject matter of the invention. The amendments to Claims 1, 11, 42 and claims dependent thereon are supported in the specification at page 30, paragraph [63], and do not constitute new matter. Claims 10, 21, 41 and dependent claims 23, 26 and 28 are currently amended to be drawn to the elected subject matter. Claims 23 and 24 are amended to be of proper dependent form. The claims are amended herein without prejudice to the prosecution of subject matter cancelled by amendment in other patent applications, and none of the amendments constitute new matter.

Claims 10, 21 and 41 are objected to for comprising subject matter drawn to a non-elected invention. Claims 22-24 are objected to as being of improper dependent form.

Claims 10, 11, 13, 14, 20-24, 30, 31, 33, 34, 40 and 41 are rejected under the first paragraph of 35 U.S.C. §112 for allegedly failing to comply with the written description requirement and for lacking enablement.

Claims 1, 3, 4, 6-11, 13, 14, 16-24, 26-31, 33, 34, and 36- 42 are rejected under the first paragraph of 35 U.S.C. §112 for alleged lack of enablement.

For reasons set forth herein, the rejections should be removed and the claims should be deemed allowable.

1. **The Claims Comply With The Original Restriction Requirement:**

Claims 10, 21, and 41 are objected to under 37 C.F.R. §1.142 (b) for failing to read on the originally elected subject matter. In particular, the Examiner notes that claims 10, 21 and 41 encompass a method for inhibiting proliferation of cancer cells via administration of an effective amount of an MDA-7 protein. The original restriction requirement required separating method claims comprising protein therapy from method claims comprising gene therapy.

Claims 10, 21 and 41, as currently amended, delete reference to direct administration of MDA-7 protein in order to comply with the original restriction requirement. The objection to Claims 10, 21 and 41 should therefore be withdrawn.

2. **The Claims Are Of Proper Dependent Form**

Claims 22-24 are objected to under 37 C.F.R. §1.75(c) as being of improper dependent form for failing to further limit the subject matter of previous claims. The Examiner states that Claim 22 drawn to a method of Claim 21 wherein the amount of MDA-7 protein is increased by introduction of nucleic acid encoding MDA-7 protein in expressible form, does not further limit Claim 22. Claims 23 and 24 depend on Claim 22, and are objected to for the same reason.

Claim 22 is cancelled. Claim 23 and Claim 24 are amended to be of proper dependent form thereby obviating the basis for this rejection, which should be withdrawn.

3. The Claims Comply With The Written Description Requirement And Are Enabled

Claims 10, 11, 13, 14, 20-24, 30, 31, 33, 34, 40 and 41 are finally rejected under 35 U.S.C. §112, first paragraph, as failing to comply with the written description requirement. The claims allegedly contain subject matter which is not described in the specification. In particular, the instant claims are said to encompass a genus of agents including anti-*ras* agents and agents that inhibit EGFR, RAF, MAPKK, MAPK and PI3K. These claims are alleged to encompass an extremely large number of molecules including as yet unidentified ones. It is further noted by the Examiner that the ribozyme and precursor of triple helix of Claims 10, 11, 21, 31 and 41 and claims dependent thereon allegedly fail to specify an anti-*ras* specific activity.

Additionally, in view of the written description rejection, Claims 10, 11, 13, 14, 20-24, 30, 31, 33, 34, 40 and 41 are rejected under 35 U.S.C. §112, first paragraph, as failing to comply with the enablement requirement. The basis of this rejection is the alleged failure to provide clear and adequate disclosure of the species of molecules encompassed by the claims. It is stated by the Examiner that without adequate disclosure of the species molecules encompassed by the claims, one skilled in the art would not know how to make or use the claimed invention without performing an undue amount of additional experimentation.

The claims are amended to specify a *ras*-specific ribozyme and a *ras*-specific precursor of triple helical molecule, thus obviating the grounds for rejection of these claims by the Examiner based on lack of specifying the "*ras*-specificity" of the inhibitors. Claims dependent on Claims 10, 11, 21, 31 and 41 *i.e.* Claims 13, 14, 16, 19 dependent on Claim 11; Claims 23 and 24 dependent on Claim 21; and Claims 33 and 34 dependent on Claim 31 are also enabled following amendment to the corresponding independent claim.

The claims are, in addition, amended to delete methods drawn to an agent which inhibits a molecule selected from a group consisting of farnesyl transferase, the epidermal growth factor receptor, RAF, MAPK kinase, MAP kinase and PI3 kinase. These amendments are made without prejudice to pursuing the deleted subject matter in other applications.

Claims 20, 30 and 40 are cancelled, thus obviating the grounds for their rejection.

The amended claims therefore comply with the written description requirement and are enabled. For these reasons, the rejection of claims 10, 11, 13, 14, 21, 23, 24, 31, 33, 34 and 41 should be removed.

4. <u>The Claims Are Enabled</u>

Claims 1, 3, 4, 6-11, 13, 14, 16-24, 26-31, 33, 34, and 36-42 are finally rejected under 35 U.S.C. §112, first paragraph, for lack of enablement. The Examiner states that the specification is enabling for:

> A method for inhibiting proliferation and/or inducing apoptosis in cancer cells wherein said cancer cells comprise a mutated ras gene that increases RAS activity in the cancer

> cell, wherein said method comprises directly administering to said cancer cells a composition comprising:
> (i) a nucleic acid that encode and expresses MDA-7 in said cancer cells, and
> (ii) an antisense nucleic acid molecule that specifically hybridizes to a nucleic acid encoding to the mutated ras gene under stringent conditions;
>
> but does not provide enablement for the full scope encompassed by the claims. The specification does not enable any person skilled in the art to make and use the invention commensurate in scope with these claims.

Further, the Examiner has objected to the term "treating" as being too broad. This term allegedly encompasses not only inhibiting growth of pancreatic cancer cells but also complete curing and preventing future occurrence of pancreatic cancer in the subject. The applicant is required to address the rejection with respect to use of the term "treating". In addition, the Examiner contends that the Applicant has not rebutted contentions previously made by the Examiner that indirect delivery of therapeutic compounds is not enabled, and claims encompassing non-*ras*-specific ribozymes or precursors of triple helixes are contended to be not fully enabled.

The Applicant respectfully asserts that the claims satisfy enablement requirements under 35 U.S.C. §112, first paragraph.

First, the Examiner has contended that the term "treating" would encompass not only inhibiting growth of pancreatic cancer cells but also complete curing and preventing future occurrence of pancreatic cancer in the subject and is therefore not enabled.

The specification states at page 44, paragraph [0098] that:

> The subject may be administered a therapeutically effective amount of a combination of MDA-7 increasing and RAS activity decreasing agents by a suitable route, including intra-tumor installation, intravenous, intraarterial, intrathecal, intramuscular, intradermal,

> subcutaneous, etc. A therapeutically effective amount of these agents produces one or more of the following results: a decrease in tumor mass, a decrease in cancer cell number, a decrease in serum tumor marker, a decrease in tumor metastasis, a decreased rate of tumor growth, improved clinical symptoms, and/or increased patient survival. The cancer may be first treated surgically to de-bulk the tumor mass, if appropriate.

As set forth above, a person skilled in the art will clearly know what the term "treating" would encompass and what effect should follow or be expected. The Applicant therefore respectfully requests that the rejection based on lack of enablement be withdrawn.

Second, the claims are rejected for alleged lack of enablement of claimed method(s) of delivery of the therapeutic compounds other than by direct delivery and the alleged unpredictability of the art encompassing gene therapy and antisense therapy.

The Applicant asserts that it would be clear to one of ordinary skill in the art to utilize the instant invention without undue experimentation because the specification and working examples provide sufficient detail to enable the instant invention. At page 44 and bridging page 45, paragraph [0099] the delivery method, alternative routes of delivery and dosage of therapeutic agents is specified. Section 5.5 "Methods of Use" at pages 44-48 and several working examples provided in Sections 6-9 at pages 48-66 discuss the variables, conditions of treatment, cell culture conditions etc. which fully enable the instant invention. The Examiner's attention is also drawn to Exhibits 1-3 which are references describing the successful utilization of Ad.mda-7 in human clinical trials or to treat systemic disease.

> Exhibit 1: Ramesh *et al.*, "Local and systemic inhibition of lung tumor growth after nanoparticle-mediated mda-7/IL-24 gene delivery" DNA Cell Biol. 2004 23(12):850-857.

Exhibit 2: Tong *et al.*, "Intratumoral injection of INGN 241, a nonreplicating adenovector expressing the melanoma-differentiation associated gene-7 (mda-7/IL24): biologic outcome in advanced cancer patients" Mol Ther. 2005 11(1):160-172.

Exhibit 3: Cunningham *et al.*, "Clinical and local biological effects of an intratumoral injection of mda-7 (IL24; INGN 241) in patients with advanced carcinoma: a phase I study" Mol Ther. 2005 11(1):149-159.

Thus, for the reasons set forth above, the Applicant respectfully requests that the rejection for alleged lack of enablement of claimed method(s) of delivery of the therapeutic compounds be withdrawn.

Third, as to the grounds of rejection for lack of enablement of ribozymes and precursors of triple-helix molecules not targeted to the RAS gene, Claims 10, 11, 21, 31 and 41 and claims dependent thereon are currently amended to specify a *ras*-specific ribozyme and a *ras*-specific precursor of triple helical molecule, thus obviating the grounds for rejection of these claims by the Examiner based on lack of specifying the "*ras*-specificity" of the inhibitors.

For all the reasons set forth above, the claims are enabled and the rejection should be withdrawn.

5. Conclusion

For all the foregoing reasons, it is respectfully requested that the rejections of the claims be withdrawn. An early allowance is earnestly requested.

Respectfully submitted,

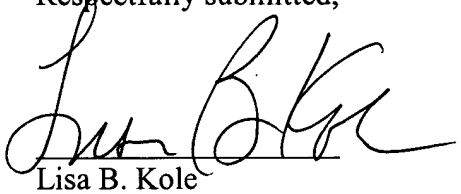

Lisa B. Kole
Reg. No. 35,225
(212) 408-2628

BAKER BOTTS L.L.P.
Attorney for Applicant

DNA AND CELL BIOLOGY
Volume 23, Number 12, 2004

Pp. 850–857

Local and Systemic Inhibition of Lung Tumor Growth After Nanoparticle-Mediated *mda-7/IL-24* Gene Delivery

RAJAGOPAL RAMESH,[1] ISAO ITO,[1] YUJI SAITO,[1] ZHENG WU,[2] ABNER M. MHASHIKAR,[2] DEBORAH R. WILSON,[2] CYNTHIA D. BRANCH,[1] JACK A. ROTH,[1] and SUNIL CHADA[2]

ABSTRACT

The human melanoma differentiation associated gene-7 (*mda-7*), also known as interleukin-24 (*IL-24*), is a novel gene with tumor suppressor, antiangiogenic, and cytokine properties. *In vitro* adenovirus-mediated gene transfer of the human *mda-7/IL-24* gene (Ad-*mda-7*) results in ubiquitous growth suppression of human cancer cells with minimal toxicity to normal cells. Intratumoral administration of Ad-*mda-7* to lung tumor xenografts results in growth suppression via induction of apoptosis and antiangiogenic mechanisms. Although these results are encouraging, one limitation of this approach is that its locoregional clinical application-systemic delivery of adenoviruses for treatment of disseminated cancer is not feasible at the present time. An alternative approach that is suitable for systemic application is non-viral gene delivery. We recently demonstrated that DOTAP:cholesterol (DOTAP:Chol) nanoparticles effectively deliver tumor suppressor genes to primary and disseminated lung tumors. In the present study, therefore, we evaluated nanoparticle-mediated delivery of the human *mda-7/IL-24* gene to primary and disseminated lung tumors *in vivo*. We demonstrate that DOTAP:Chol efficiently delivers the *mda-7/IL-24* gene to human lung tumor xenografts, resulting in suppression of tumor growth. Growth-inhibitory effects were observed in both primary ($P = 0.001$) and metastatic lung tumors ($P = 0.02$). Furthermore, tumor vascularization was reduced in *mda-7/IL-24*–treated tumors. Finally, growth was also inhibited in murine syngenic tumors treated with DOTAP:Chol–*mda-7* nanoparticles ($P = 0.01$). This is the first report demonstrating (1) systemic therapeutic effects of *mda-7/IL-24* in lung cancer, and (2) antitumor effects of human *mda-7* in syngeneic cancer models. Our findings are important for the development of *mda-7/IL-24* treatments for primary and disseminated cancers.

INTRODUCTION

THE HUMAN MELANOMA DIFFERENTIATION associated gene-7 (*mda-7*), also known as interleukin-24 (*IL-24*), is a novel gene that was identified in human melanoma cells (Jiang *et al.*, 1995). Expression of *mda-7* mRNA has been reported in normal melanocytes and early stages of melanoma, but not in cell lines derived from advanced tumors, suggesting that *mda-7* is a novel tumor suppressor gene whose expression must be inhibited for tumor progression. Furthermore, restoration of human *mda-7* gene expression in tumor cells resulted in suppression of tumor growth (Jiang *et al.*, 1996; Su *et al.*, 1998). In recent studies, MDA-7 protein expression was demonstrated in early stages of melanomas but not in advanced melanomas (Ekmekcioglu *et al.*, 2001; Ellerhorst *et al.*, 2002). These studies firmly established an inverse correlation between MDA-7 protein expression and melanoma disease progression. Analysis of human tumors from lung, breast, and colorectal carcinomas and sarcoma confirm the lack of MDA-7 expression in human tumors (Chada *et al.*, 2004). These results suggested that MDA-7 plays an important role in the development and/or progression of human cancers. Using adenoviral vectors, ectopic expression of human MDA-7/IL-24 in a wide variety of human cancer cells results in ubiquitous growth suppression and apoptotic cell death (Jiang *et al.*, 1996; Su *et al.*, 1998; Saeki *et al.*, 2000; Mhashilkar *et al.*, 2001; Cao *et al.*, 2002; Lebedeva *et*

[1]Department of Thoracic and Cardiovascular Surgery, The University of Texas M.D. Anderson Cancer Center, Houston, Texas.
[2]Introgen Therapeutics Inc., Houston, Texas.

al., 2002; Fisher *et al.*, 2003; Kawabe *et al.*, 2002; Gopalan *et al.*, 2003; Saito *et al.*, 2003; Yacoub *et al.*, 2003a, 2003b). MDA-7 does not, however, exhibit any significant cytotoxicity to normal cells. Thus, *mda-7* exerts its growth-inhibitory effects selectively in human tumor cells but not in normal cells. The mechanism by which *mda-7* induces tumor cell apoptosis varies, and appears to be cell-type dependent. A number of molecular effectors have been shown to play a role in *mda-7*–mediated apoptosis including activation of the caspase cascade (Saeki *et al.*, 2000, 2002), activation of PKR (Pataer *et al.*, 2002), activation of p38MAPK (Sarkar *et al.*, 2002a, b), inhibition of PI3K survival signaling (Mhashilkar *et al.*, 2003), activation of the UPR stress response (Sieger *et al.*, 2004), and activation of Fas-FasL (Gopalan *et al.*, unpublished data). Although the upstream signaling pathways utilized by *mda-7* vary among the different tumor types tested, the pathways clearly converge downstream at the level of mitochondrial disruption, resulting in tumor cell death. The results of these studies have established *mda-7* as a novel therapy for cancer.

More recently, we demonstrated that the MDA-7 protein is secreted (Mhashilkar *et al.*, 2001) and that the secreted MDA-7/IL-24 (sMDA-7/IL-24) protein has potent antiangiogenic activity (Ramesh *et al.*, 2003). In a separate study, Caudell *et al.* (2002) demonstrated that sMDA-7/IL-24 protein functions as a pro-Th1 cytokine. Thus, human *mda-7* is an unusual and novel molecule with multiple functions that include antitumor, antiangiogenic, and cytokine activities. On the basis of its unique properties, a phase I clinical trial of *mda-7* for treatment of patients with solid tumors has been completed. In this study, an adenoviral vector containing the human *mda-7* gene (Ad-*mda-7*; INGN241) was administered intratumorally to 22 patients. Preliminary results indicated that Ad-*mda-7* was well tolerated with no toxic effects and induced high levels of apoptosis in tumors (Chada *et al.*, 2003). Although these results are encouraging, a major limitation of this approach is its locoregional application. Systemic use of high-dose adenovirus-based gene therapy vectors for treatment of metastatic cancers is currently limited by several factors, including induction of immune response against the vector and potential for liver toxicity (Varnavski *et al.*, 2002; Vlachaki *et al.*, 2002). Therefore, there is a need to develop and test alternate vector systems that can deliver the *mda-7* gene systemically to disseminated cancers.

One delivery system that may effectively deliver the human *mda-7* gene to disseminated tumors is the cationic DOTAP:cholesterol nanoparticle (DOTAP:Chol). We recently demonstrated that DOTAP:Chol efficiently delivers tumor suppressor genes to primary and disseminated lung cancers with minimal toxicity (Ramesh *et al.*, 2001). Furthermore, a DOTAP:Chol–DNA complex was selectively taken up by lung tumors *in situ*, resulting in greatly increased transgene expression in the tumors compared to surrounding normal lung tissue (Ito *et al.*, 2003). We therefore evaluated DOTAP:Chol-mediated human *mda-7* gene delivery to primary and disseminated lung tumors in both immunodeficient, and immunocompetent murine models. In the present study, we demonstrate that DOTAP:Chol nanoparticle effectively delivered the human *mda-7/IL-24* gene to primary and disseminated human lung tumor xenografts, resulting in suppression of tumor growth. Similar results were also observed in syngeneic tumor models, demonstrating for the first time that human *mda-7* can exert its antitumor activity in murine tumors established in immunocompetent mice. These results indicate that DOTAP:Chol nanoparticle-mediated *mda-7* gene delivery is a novel strategy for treatment of disseminated cancer.

MATERIALS AND METHODS

Materials

All lipids (DOTAP, cholesterol) were purchased from Avanti Polar Lipids (Albaster, AL). Ham's/F12 medium and fetal bovine serum (FBS) were purchased from GIBCO-BRL-Life Technologies (New York, NY). Polyclonal rabbit antihuman MDA-7 antibody was obtained from Introgen Therapeutics, Inc. (Houston, TX) and antimouse CD31 from Santa Cruz Biotechnology, Inc. (Palo Alto, CA).

Cell lines and animals

Human nonsmall cell lung carcinoma cell line A549 was obtained from American Type Culture Collection (Rockville, MD) and maintained in Ham's-F12 medium supplemented with 10% FBS, 1% glutamate, and antibiotics. Murine UV2237M cells were obtained from Dr. Isaiah J. Fidler (M.D. Anderson Cancer Center) and maintained as described elsewhere (Ramesh *et al.*, 2001). Cells were regularly passaged and tested for presence of mycoplasma. Four- to 6-week-old female BALB/c nude (*nu/nu*) mice (Harlan–Sprague–Dawley Inc., Indianapolis, IN) and C3H/Ncr mice (National Cancer Institute, Fredericksburg, MD) used in the study were maintained in a pathogen-free environment and handled according to institutional guidelines established for animal care and use.

Purification of plasmids

The plasmids used in the study were cloned in pVax plasmid vector (Invitrogen, Carlsbad, CA) and purified as described elsewhere (Templeton *et al.*, 1997; Gaensler *et al.*, 1999). Briefly, plasmids carrying the bacterial β-galactosidase (*Lac-Z*), chloramphenicol acetyl transferase (*CAT*), or human *mda-7* cDNA, under the control of cytomegalovirus (*CMV*) promoter, were grown under kanamycin selection in the *Escherichia coli* host strain DH5α. Endotoxin levels of purified plasmids were determined by using the chromogenic limulus amebocyte lysate kinetic assay kit (Kinetic-QCL; Biowhittaker, Walkersville, MD). The concentration and purity of the purified plasmid DNA's were determined by OD 260/280 ratios.

Synthesis of DOTAP:Chol nanoparticles and preparation of DOTAP:Chol–DNA nanoparticles

DOTAP:Chol nanoparticles were synthesized and extruded through Whatman filters (Kent, UK) of decreasing size (1.0, 0.45, 0.2, and 0.1 μm) as described elsewhere (Chada *et al.*, 2003; Templeton *et al.*, 1997). DOTAP:Chol–DNA nanoparticles were prepared fresh 2 to 3 h prior to injection in mice.

Particle size analysis

Freshly prepared DOTAP:Chol–DNA nanoparticles were analyzed for mean particle size by using the N4 particle size analyzer (Coulter, Miami, FL). The mean particle size of the DOTAP:Chol–DNA nanoparticles ranged between 300 and 325 nm.

Effect of the DOTAP:Chol-mda7 *nanoparticles on subcutaneous tumor xenografts*

In all the experiments, 5×10^6 tumor cells (A549) suspended in 100 μl sterile phospate-buffered saline (PBS) were injected into the right dorsal flank. When the tumors reached a size of 4–5 mm^2, the animals were randomized into groups and treatment was initiated. Tumor-bearing animals were divided into four groups of six animals. Group 1 received no treatment, group 2 received PBS, group 3 received DOTAP:Chol–*LacZ* nanoparticles (50 μg/dose), and group 4 received the DOTAP:Chol–*mda-7* nanoparticles (50 μg/dose); all treatments were administered intratumorally and were given daily for a total of six doses. Animals were anesthetized with methoxyflurane (Schering-Plough, Kenilworth, NJ) for intratumoral injections per institutional guidelines. Tumor measurements were recorded every other day by observers without knowledge of the treatment groups, and tumor volumes were calculated by using the formula V (mm^3) = $a \times b^2/2$, where a is the largest dimension and b is the perpendicular diameter (Ramesh *et al.*, 2001; Saeki *et al.*, 2002). Antitumor efficacy data are presented as cumulative tumor volumes for all animals in each group to account for both size and number of tumors. In all experiments, the statistical significance of changes in tumor size was determined on days 21 and 24 by ANOVA.

To test the effect of *mda-7* on mouse tumor cells, we utilized a syngeneic tumor model. For this purpose, C3H mice were injected subcutaneously with murine UV2237m fibrosarcoma cells (1×10^6) and divided into three groups (n = 8/group). When the tumor size reached 4–5 mm^{2-}, animals received intratumoral treatment as follows: no treatment (control), DOTAP:Chol–*CAT* nanoparticles, or DOTAP:Chol–*mda-7* nanoparticles. Treatment schedule and analyses of the therapeutic effects were the same as already described for the A549 tumor model. Experiments were repeated two times for statistical analysis and significance calculated on days 21 and 23 by ANOVA.

Measurement of MDA-7, apoptosis, and CD31

Subcutaneous A549 or UV2237m tumors established in *nu/nu* or C3H mice, respectively, were harvested and fixed in 4% buffered formalin, embedded in paraffin, and cut in 4-μm sections. Tissue sections were immunostained for MDA-7 transgene expression as described elsewhere (Saeki *et al.*, 2002; Ramesh *et al.*, 2003). The tumor cells staining positive for *mda-7* were analyzed under bright-field microscopy and quantitated by observers without knowledge of the treatment groups. At least five fields per specimen were analyzed. To determine the fate of tumor cells following treatment, sections of tumors were stained for apoptotic cell death with terminal deoxynucleotide transferase (Tdt) kit (Boehringer Mannheim, Indianapolis, IN) and counterstained with methylene blue or methyl green as described previously (Ramesh *et al.*, 2001; Saeki *et al.*, 2002). In all staining procedures, appropriate negative controls were included. For CD-31 staining, tissues were stained with anti-CD31 antibody as described previously (Saeki *et al.*, 2002; Ramesh *et al.*, 2003) and observed under a microscope in a blind fashion. Microvessel density (MVD) was determined semiquantitatively by counting the number of CD31-positive staining vessels in five randomly selected fields per tumor tissue under high-power magnification (×400). A total of 15 fields representing three tumor tissues per treatment group was examined and quantitated, and the results represented as the average number of vessels per field.

Tumor characteristics after treatment

To determine the therapeutic effects of the *mda-7* gene, tumors were harvested from mice after the last treatment and subjected to histopathologic examination. Analysis was done by a pathologist without prior knowledge of the treatment groups.

Effect of the DOTAP:Chol–mda7 *nanoparticles on experimental lung metastasis*

To test the effect of the DOTAP:Chol–*mda-7* nanoparticles on lung metastases, female nude mice were injected via tail vein with 10^6 A549 tumor cells suspended in 100 μl of sterile PBS. Six days later, the mice were divided into three groups and treated as follows: no treatment (group 1), DOTAP:Chol–*CAT* nanoparticles (group 2), and DOTAP:Chol–*mda-7* nanoparticles (group 3). There were eight mice in each group. All treatments comprised of 50-μg nanoparticles–DNA and were administered daily via tail vein using a 27-gauge needle for a total of six doses. Three weeks following the last dose, animals were euthanized by CO_2 inhalation. The lungs of each mouse were injected intratracheally with India ink and fixed in Feketes solution (Ramesh *et al.*, 2001). The therapeutic effects of systemic *mda-7* gene treatment were determined by counting the number of metastatic tumors in each lung under a dissecting microscope by an observer without knowledge of the treatment groups. The data were analyzed, and differences among groups were interpreted as statistically significant if the P-value was <0.05 by the Mann-Whitney rank-sum test.

As a syngeneic lung tumor model, C3H mice were injected with murine UV2237m fibrosarcoma cells (1×10^6) and divided into three groups (n = 7/group). Six days after injection, animals were treated as follows: no treatment, DOTAP:Chol–*CAT* nanoparticles, or DOTAP:Chol–*mda-7* nanoparticles. Treatment schedule and analyses of therapeutic effect were the same as already described for the A549 models. Experiments were performed two times for statistical significance.

RESULTS

In vitro *transfection of tumor cells with DOTAP:Chol*-mda-7 *nanoparticles*

We determined the ability of DOTAP:Chol nanoparticles to deliver plasmid DNA into human (A549) and mouse (UV2237m) tumor cells by using expression plasmids encoding the human MDA-7/IL-24 protein. Transfection with DOTAP:Chol nanoparticles complexed with *mda-7* plasmid DNA, resulted in expression of exogenous MDA-7 protein in both A549 and UV2237m tumor cells at 24 and 48 h (Fig. 1A). MDA-7 expression was not observed in PBS-treated control cells. Analysis of tissue culture supernatant from DOTAP:Chol-*mda-7* transfected A549 and UV2237m cells showed secreted MDA-7 protein at 48 h but not at 24 h (Fig. 1B). Detection of secreted MDA-7 protein at 48 h is unlike that observed in Ad-*mda7*–treated cells where secreted MDA-7 protein is detectable

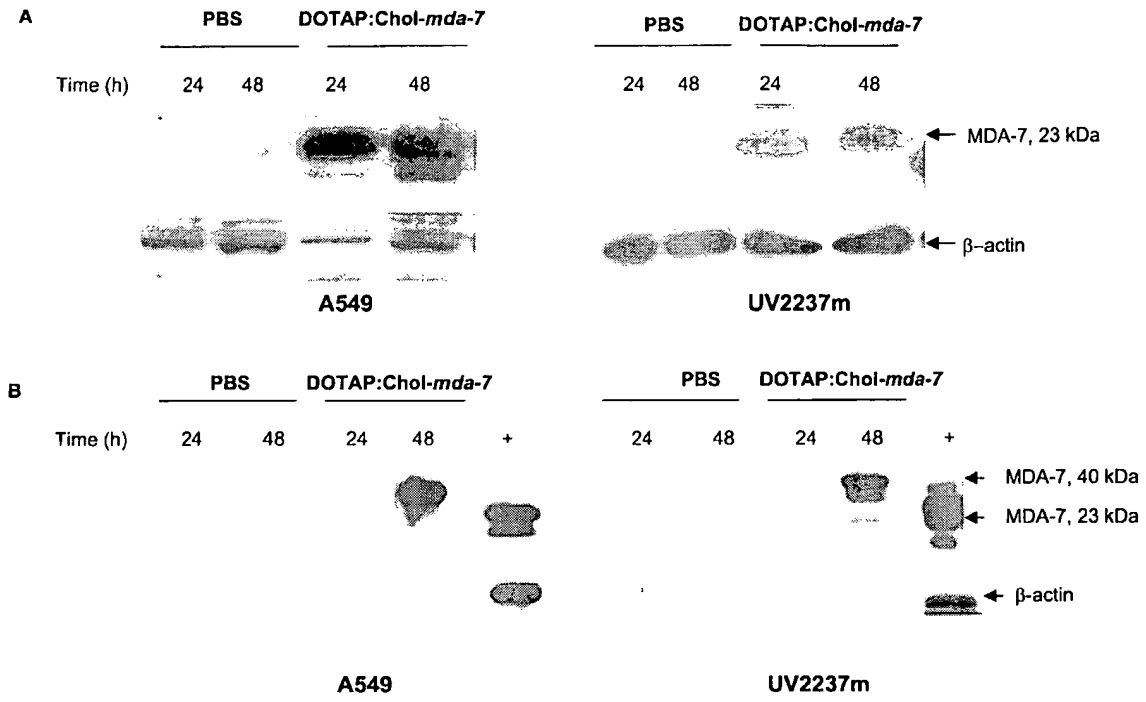

FIG. 1. *In vitro* expression of MDA-7. Tumor (A549, and UV2237m) cells transfected with a DOTAP:Chol–*mda-7* nanoparticles were analyzed for MDA-7 protein expression at 24 and 48 h after transfection. PBS treated cells served as a control. β-Actin was used a loading control in western blotting. (**A**) MDA-7 protein expression was detected in cell lysates that were prepared from cells transfected with a DOTAP:Chol–*mda7* nanoparticles but not in PBS-treated cells. Expression was observed at all time points tested. (**B**) Analysis of tissue culture supernatants showed secreted MDA-7 protein (40 kDa) from DOTAP:Chol–*mda-7* nanoparticles with transfected A549 and UV2237m cells. Secreted MDA-7 protein was not detected in PBS treated cells. β-Actin served as loading controls. (+) denotes positive control for intracellular MDA-7 protein (23 kDa).

at 24 h (Mhashilkar *et al.*, 2001). This suggests that the transgenic MDA-7 expression achieved using the DOTAP:Chol nanoparticles is less than that obtained with Ad-*mda-7*. Secreted MDA-7 protein was not observed in PBS-treated cells. Thus, DOTAP:Chol nanoparticles could effectively deliver *mda-7* DNA to tumor cells resulting in intracellular and secreted transgenic MDA-7 production, albeit less than Ad-*mda-7*.

MDA-7 inhibits subcutaneous tumor growth

We assessed the ability of the DOTAP:Chol–*mda-7* nanoparticles to suppress the growth of A549 human lung subcutaneous tumors in *nu/nu* mice. Treatment of tumor-bearing mice with the DOTAP:Chol–*mda-7* nanoparticles via the intratumoral route significantly inhibited tumor growth ($P = 0.001$) compared with tumor growth in animals that were untreated, treated with PBS, or treated with the DOTAP:Chol–*LacZ* nanoparticles (Fig. 2A). Histopathological analysis of the tumors revealed no significant changes in the tumor infiltrating cells among the various treatment groups (data not shown).

The therapeutic effects of the *mda-7* gene on subcutaneous murine tumors in C3H mice were next evaluated. Mice bearing UV223M tumors were divided into three groups, one receiving no treatment, a second receiving treatment with the DOTAP:Chol–*CAT* nanoparticles, and a third receiving treatment with the DOTAP:Chol–*mda-7* nanoparticles. Growth of UV2237m tumors was inhibited starting from day 19 in mice treated with intratumoral administration of the DOTAP:Chol–*mda-7* nanoparticles when compared with tumor growth in the two control groups (Fig. 2B). However, significant tumor inhibition was observed on day 23 ($P = 0.01$). Tumor inhibition ($P = 0.24$) was also observed in mice treated with the DOTAP:Chol–*CAT* nanoparticles compared to untreated control mice. However, the inhibitory effect observed in the DOTAP:Chol–*CAT* nanoparticle-treated mice is attributed to nonspecific effects, and is in agreement with our previous studies (Ramesh *et al.*, 2001).

To demonstrate that the observed tumor-suppressive effects was due to *mda-7* gene expression, subcutaneous A549 and UV2237m tumors obtained at 48 h after injection were subjected to immunohistochemical analysis for MDA-7 protein expression. MDA-7 protein expression was seen in 18 and 13% of A549 and UV223m tumors, respectively, which were treated with the DOTAP:Chol–*mda-7* nanoparticles ($P = 0.001$; Fig. 2C), a significantly higher number than in the animals that were not treated, treated with PBS, treated with DOTAP:Chol–*LacZ*, or treated with the DOTAP:Chol–*CAT* nanoparticles. Some level of nonspecific staining was observed in A549 tumors that were treated with the DOTAP:Chol–*CAT* nanoparticles. Analysis of the pattern of MDA-7 expression revealed intense intracellular staining in ad-

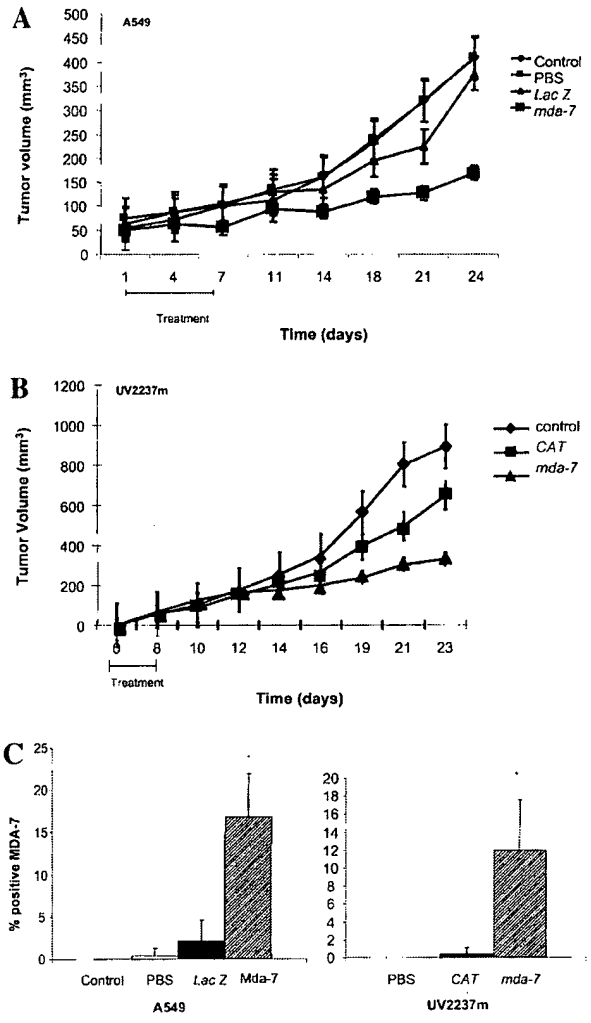

FIG. 2. DOTAP:Chol–*mda-7* nanoparticles suppresses growth of subcutaneous tumors. Subcutaneous tumor-bearing (A549 or UV223m) nude mice and C3H mice were divided into groups and treated daily for a total of six doses (50 μg/dose), as follows: no treatment, PBS, DOTAP:Chol-*LacZ* nanoparticles or, DOTAP:Chol–*CAT* nanoparticles, and DOTAP:Chol–*mda-7* nanoparticles. (**A**) A549. (**B**) UV2237m. Each time point represents the mean tumor volume for each group. Bars represent standard errors. (**C**) Subcutaneous tumors were harvested 48 h after treatment and analyzed for MDA-7 protein expression. In tumors treated with the DOTAP:Chol–*mda-7* complex, 18% of A549 tumor cells and 13% of UV2237m tumor cells produced the MDA-7 protein, while control tumors produced no MDA-7 protein.

dition to a more diffuse staining pattern that appeared to be extracellular. This pattern of staining was observed in both human tumor xenografts and murine syngeneic tumors. (data not shown).

*Apoptotic cell death in lung tumors treated with DOTAP:Chol–*mda-7 *nanoparticles*

To determine the fate of tumor cells after treatment with the DOTAP:Chol–*mda-7* complex, subcutaneous tumors (A549, UV2237m) from *nu/nu* mice and C3H mice were analyzed for apoptotic cell death as previously described (Saeki *et al.*, 2002). A significant ($P = 0.001$) level of TUNEL positive cells (13% A549, and 9% UV2237m) indicative of apoptotic cell death was observed in tumors treated with DOTAP:Chol–*mda-7* nanoparticles compared to tumors from control animals that were untreated, treated with PBS, treated with DOTAP:Chol–*CAT* or treated with DOTAP:Chol–*LacZ* nanoparticles (Fig. 3).

*Reduced CD31-positive staining in lung tumors treated with a DOTAP:Chol–*mda-7 *nanoparticles*

To determine the effect of *mda-7* treatment on tumor vascularization, tumor tissues were subjected to CD31 staining as previously described (Saeki *et al.*, 2002; Ramesh *et al.*, 2003). Levels of CD31-positive staining was significantly ($P = 0.01$) reduced in DOTAP:Chol–*mda7* treated A549 (10%) and UV2237m (5.8%) tumor tissues compared to tumor tissues obtained from untreated, PBS-treated, DOTAP:Chol–*LacZ* treated, and DOTAP:Chol–*CAT*- treated mice (Fig. 4). Reduced CD31 staining is indicative of reduced vascularization.

MDA-7 inhibits experimental lung metastases

The activity of DOTAP:Chol–*mda-7* nanoparticles was next investigated in an experimental lung metastases model using human A549 lung cancer cells or mouse UV227m cells. Intravenous delivery of tumor cells results in rapid tumor seeding of lungs, and animals succumb to overwhelming lung tumor burden after 30 days. Systemic treatment of A549 and UV2237m lung tumor-bearing nude or C3H mice with the DOTAP:Chol–*mda-7* nanoparticles resulted in a significantly ($P < 0.05$) lower number of lung metastases than treatment with PBS or the DOTAP:Chol–*CAT* nanoparticles (Fig. 5). In UV2237m mice, treatment with the DOTAP:Chol–*CAT* nanoparticles resulted in a significant reduction in the number of tumor nodules when compared to those treated with PBS suggesting some nonspecific antitumor activity (Fig. 5). Furthermore, the treatment was well tol-

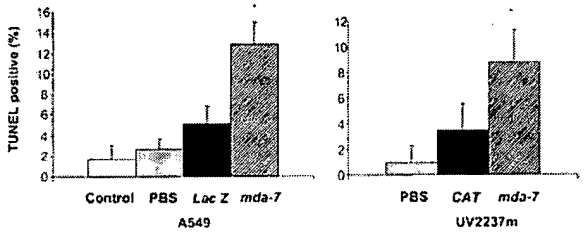

FIG. 3. MDA-7 induces apoptotic cell death following treatment with the DOTAP:Chol–*mda-7* nanoparticles. Subcutaneous tumors (A549, and UV2237m) from animals receiving no treatment, PBS, a DOTAP:Chol–*LacZ*, or DOTAP:Chol–*CAT* nanoparticles, or the DOTAP:Chol–*mda-7* nanoparticles were harvested and analyzed for apoptotic cell death by TUNEL staining. The percentages of cells undergoing apoptotic cell death (13% for A549 and 9% for UV2237m) in tumors treated with the DOTAP:Chol–*mda-7* nanoparticles were significantly higher ($P = 0.001$) than in the other treatment groups. Bars denote standard deviation.

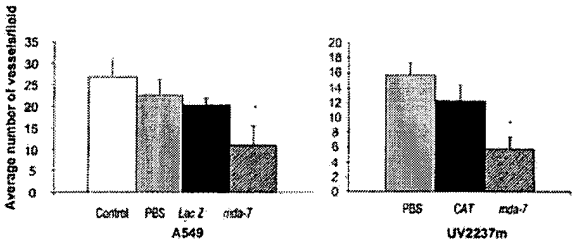

FIG. 4. DOTAP:Chol–*mda-7* nanoparticles inhibit tumor vascularization.Subcutaneous tumors (A549, and UV2237m) that were either untreated or treated with PBS, a DOTAP:Chol–*LacZ*, or DOTAP:Chol–*CAT* nanoparticles, or DOTAP:Chol–*mda-7* nanoparticles were stained for CD31 and subjected to semiquantitative analysis. CD31–positive endothelial staining was significantly lower ($P = 0.01$) in DOTAP:Chol–*mda7*-treated tumors than in the tumors of other treatment groups. Bars denote standard deviation.

erated with no treatment related toxicity observed as evidenced by lack of morbidity and mortality.

DISCUSSION

We have previously demonstrated that adenovirus-mediated transfer of the *mda-7* gene (Ad-*mda7*) to human lung cancer cells results in suppression of growth and induction of apoptosis, both *in vitro* and *in vivo* (Saeki *et al.*, 2000, 2002; Mhashilkar *et al.*, 2001). Furthermore, we recently demonstrated that secreted MDA-7 protein possesses potent antiangiogenic activity and was 20–50-fold more potent than the antiangiogenic proteins, endostatin, and angiostatin (Ramesh *et al.*, 2003). Collectively, these data indicate that *mda-7* is a novel therapeutic agent with antitumor and antiangiogenic properties. A phase I clinical trial for treatment of solid tumors was initiated using Ad-*mda-7*/INGN241 (Chada *et al.*, 2001, 2003). In this trial, patients were treated by intratumoral administration of Ad-*mda-7*. A rigorous pharamacokinetic and pharmacodynamic analysis of intratumoral vector distribution was performed. Vector-specific DNA, RNA, transgenic MDA-7 protein, and biological activities were evaluated in tumors resected at various times after Ad-*mda-7* injection. The resected patient tumors exhibited high levels of transgenic MDA-7 protein that correlated geographically with TUNEL signals. Intratumoral vector DNA and RNA levels were quantitated and showed an intratumoral distribution of greater than 1 cm from the injection site. In contrast, MDA-7 protein and apoptosis were demonstrated at least 3 cm from the injection site, consistent with protein secretion from transduced cells. The data suggest biological activity (apoptosis induction) is more broadly distributed than vector genomes (Tong *et al.*, unpublished data). A number of patients were evaluated for clinical activity. Of five patients enrolled in a repeat dosing cohort, two showed tumor response after intratumoral injection of Ad-*mda-7*. One patient showed a complete regression of the first injected lesion and a PR of the second lesion (Cunningham *et al.*, unpublished data). This limited data set in 22 patients is encouraging, and indicates that *mda-7* gene transfer to humans is safe, and appears to exhibit biologic and clinical activity. These encouraging results suggest that Ad-*mda-7* may be an effective therapeutic agent for treatment of solid tumors. However, adenovirus gene delivery strategies are currently limited to treatment of localized disease and have not shown efficacy against disseminated disease. To overcome the limitations of adenoviral vectors, we developed cationic DOTAP:Chol nanoparticle vector as an *mda-7* gene delivery vehicle for systemic therapy. In the present study, we demonstrate that DOTAP:Chol nanoparticles effectively deliver the *mda-7/IL-24* gene to subcutaneous tumors, resulting in tumor growth suppression via induction of apoptosis and antiangiogenic mechanisms. Suppression after intratumoral administration of *mda-7* plasmid DNA is consistent with our previous studies of intratumoral injection of Ad-*mda-7* (Saeki *et al.*, 2002). It is important to note that plasmid mediated gene delivery, is much less efficient than adenoviral delivery, and also that the levels of transgene expression from plasmid DNA are orders of magnitude less than observed with Ad vectors. Given these limitations, we find significant levels of transgenic MDA-7 intratumorally and these levels are sufficient to initiate the apoptotic cascade. Others have suggested that low levels of MDA-7 are involved in its immune activity and supraphysiologic levels, such as those attained with Ad gene delivery are required for apoptosis (Fisher *et al.*, 2003; Sarkar *et al.*, 2002a). Our data are clearly inconsistent with this model, as local and systemic plasmid-mediated gene delivery results in both apoptosis and antiangiogenic effects.

In the present study, we also demonstrated for the first time the ability of *mda-7* to inhibit murine tumor growth in a syngeneic tumor model. The antitumor activity of *mda-7* has been observed in rat cells *in vitro* (Madireddi *et al.*, 2000; Chen *et al.*, 2003). We have observed *mda-7*–mediated cytotoxicity in three additional murine tumor cell lines with minimal toxicity to normal murine cells *in vitro* (Miyahara *et al.*, unpublished data). These results demonstrate that human *mda-7* also can also exert its tumor-suppressive activity against murine tumor cells and in syngeneic tumor models. The murine mda-7 was recently cloned, termed FISP, and was identified as a Th2-type cytokine

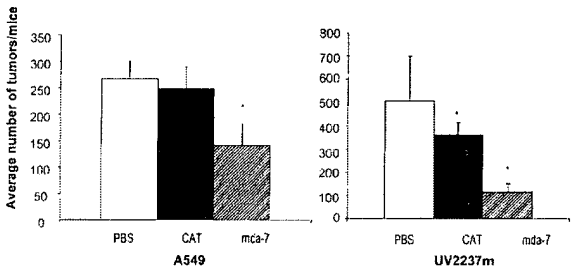

FIG. 5. DOTAP:Chol–*mda-7* nanoparticles inhibits experimental lung metastases. (**A**) Lung tumor (A549, UV2237m)-bearing *nu/nu* or C3H mice were treated daily for a total of six doses (50 μg/dose) with PBS, DOTAP:Chol–*CAT* nanoparticles, or DOTAP:Chol–*mda-7* nanoparticles. Metastatic tumor growth was significantly inhibited ($P \leq 0.05$) in both nude mice and C3H mice that were treated with DOTAP:Chol–*mda-7* nanoparticles compared with that in the two control groups. Bars denote standard deviation.

(Schaefer *et al.*, 2001). The human and murine *mda-7* genes share 80% identity and the corresponding proteins share 69%. The Th2-type cytokine activity exhibited by murine MDA-7 protein is in contrast to the Th1-type activities exhibited by human MDA-7/IL-24. Although these proteins share 69% homology, the human protein clearly functions in murine tumor and normal endothelial cells. Whether murine MDA-7 protein functions on human cells is unknown and is yet to studied. The findings from the present study provide an opportunity to conduct additional therapeutic studies in an immunocompetent setting.

The observation that *mda-7*-treated tumors had significantly reduced vascularization than control tumors indicates substantial antiangiogenic activity after plasmid delivery in xenograft and syngeneic models. This result is consistent with our previous reports demonstrating antiangiogenic activity after Ad-*mda*-7 gene delivery or MDA-7 protein treatment of human cells (Saeki *et al.*, 2002; Fisher *et al.*, 2003; Ramesh *et al.*, 2003). We have recently demonstrated downregulation of TGF-β, VEGF, FGF, and IL-8 expression in Ad-*mda*-7–treated human lung tumors (Saeki *et al.*, 2002; Nishikawa *et al.*, 2003). MDA-7 protein acts to inhibit angiogenesis in human endothelial cells via the IL-22 receptor (Ramesh *et al.*, 2003). We have now shown that MDA-7 can also inhibit angiogenesis in murine endothelial cells (data not shown). We speculate that the inhibition of tumor vascularization *in situ* is due to both a direct antiangiogenic effect of MDA-7 protein in addition to down-regulation of angiogenic growth factors. We are currently examining these possibilities in the laboratory.

It is clear that more effective treatment strategies are needed for systemic treatment of disseminated diseases, such as cancers of the lung, breast, and colon. We therefore evaluated the ability of the nanoparticles to deliver *mda-7* in disseminated lung tumors of murine and human origin. Intravenous treatments with DOTAP:Chol–*mda7* nanoparticles resulted in a reduction in the number of experimental lung tumors. Moreover, we observed no resistance to repeated treatments in agreement with our previous studies (Ramesh *et al.*, 2001; Ito *et al.*, 2003, 2004). This study clearly demonstrates for the first time the ability of intravenously delivered DOTAP:Chol–*mda-7* nanoparticles to inhibit experimental lung metastasis in both immunodeficient and immunocompetent animals. Thus, systemic delivery of human *mda-7* is feasible, and can be used to treat disseminated cancers. The combination of pro-apoptotic and antiangiogenic activities of *mda-7* coupled to systemic delivery is an exciting advance in the goal to develop effective low toxicity cancer therapeutics.

ACKNOWLEDGMENTS

The authors thank Kathryn Hale for editorial assistance and Alma Vega for preparation of this manuscript. This work was supported in part by NCI Grants R01 CA102716 to R.R.; CA89778, CA88421, and CA097598 to S.C., the Texas Higher Education Coordinating Board ATP/ARP Grant 003657-0078-2001 to R.R., by The University of Texas M.D. Anderson Cancer Center Institutional Grant (R.R.), by the W.M. Keck Gene Therapy Grant (R.R.), by NIH Cancer Center Support (CORE) Grant CA 16672, and by a sponsored research agreement with Introgen Therapeutics, Inc.

REFERENCES

CAO, X.X. MOHUIDDIN, I., CHADA, S., MHASHILKAR, A.M., OZVARAN, M.K., MCCONKEY, D.J., MILLER, S.D., DANIEL, J.C., and SMYTHE, W.R. (2002). Adenoviral transfer of mda-7 leads to BAX up-regulation and apoptosis in mesothelioma cells, and is abrogated by over-expression of BCL-XL.. Mol. Med. **8,** 869–876.

CAUDELL, E.G, MUMM J. B, POINDEXTER N, EKMEKCIOGLU S., MHASHILKAR A.M., YANG X.H., RETTER M.W., HILL P., CHADA S., and GRIMM, E.A. (2002). The protein product of the tumor suppressor gene, melanoma differentiation-associated gene 7, exhibits immunostimulatory activity and is designated IL-24. J. Immunol. **168,** 6041–6046.

CHADA, S., NEMUNAITIS, J., TONG, A., ZHANG, Y., SU, D., MHASHILKAR, A., ZHOU-YANG, H., PARKER, K., WILSON, D., MERRITT, J., *et al.* (2001). A phase I dose-escalation study of Ad-*mda7* (INGN 241) in patients with advanced carcinoma. Cancer Gene Ther. **8,** (S3), 2001.

CHADA, S., CUNNINGHAM, C., ZHANG, Y., SU, D., MHASHILKAR, A., EKMEKCIOGLU, S., GRIMM, E., WILSON, D., MERRITT, J. COFFEE, K. *et al.* (2003). INGN 241 (Ad-mda7) induces widespread apoptosis and activates the immune system in patients with advanced cancer. Mol. Ther. **7,** S446.

CHADA, S., SUTTON, R.B., EKMEKCIOGLU, S., ELLERHORST, J., MUMM, J.B., LEITNER, W., YANG H-Y, SAHIN, A.A., HUNT, K.K., RAMESH, R., *et al.* (2004). MDA-7/IL-24 is a unique cytokine-tumor suppressor in the IL-10 family. Int. Immunopharmacol. **4,** 649–667.

CHEN, J., CHADA, S., MHASHILKAR, A.M., and MIANO, J.M. (2003). Tumor suppressor *mda-7*/IL-24 selectively inhibits vascular smooth muscle cell growth and migration. Mol. Ther. **8,** 220–229.

EKMEKCIOGLU, S, ELLERHORST, J., MHASHILKAR, A.M., SAHIN A.A., READ, C.M., PRIETO V.G., CHADA, S., and GRIMM, E.A., (2001). Down-regulated melanoma differentiation associated gene (*mda-7*) expression in human melanomas. Int. J. Cancer **94,** 54–59.

ELLERHORST, J.A., PRIETO V.G., EKMEKCIOGLU, S., BROEMELING, L., YEKELL, S., CHADA S., and GRIMM, E.A. (2002). Loss of *mda-7* expression with progression of melanoma. J. Clin. Oncol. **20,** 1069–1074.

FISHER, P.B., GOPALKRISHNAN, R.V., CHADA, S., RAMESH, R., GRIMM, E.A., ROSENGELD, M.R., CURIEL, D.T., and DENT, P. (2003). *mda-7*/IL-24, novel cancer selective apoptosis inducing cytokine gene: From the laboratory into the clinic. Cancer Biol. Ther. **2,** S23–S37.

GAENSLER, K.M., TU, G, BRUCH, S., LIGGITT, D., LIPSHUTZ, G.S., METKUS, A., HARRISON, M., HEATH, T.D., and DEBS, R.J. (1999). Fetal gene transfer by transuterine injection of cationic liposome-DNA complexes. Nat. Biotechnol. **17,** 1188–1192.

GOPALAN, B., SAITO, Y., SHARMA, S., BRANCH, C.D., MHASHILKAR, A.M., ROTH, J.A., CHADA, S., and RAMESH, R. (2003). Gene therapeutic approach for treatment of human ovarian cancer using *mda-7*/IL-24. Proc. Am. Assoc. Cancer Res. **44,** 331.

ITO, I., BEGAN, G., MOHIUDDIN, I., SAEKI, T., SAITO, Y., BRANCH, C.D., VAPORCIYAN, A., STEPHENS, L.C., YEN, N., ROTH, J.A., *et al.* (2003). Increased uptake of liposomal-DNA complex by lung metastases following intravenous administration. Mol. Ther. **7,** 409–418.

ITO, I., SAEKI, T., MOHUIDDIN, I., SAITO, Y., BRANCH, C.D., VAPORCIYAN, A., ROTH, J.A., and RAMESH, R. (2004). Persistent transgene expression following intravenous administration of a liposomal complex: role of IL-10 mediated immune suppression. Mol. Ther. **9,** 318–327.

JIANG, H., LIN, J.J., SU, Z.Z., GOLDSTEIN, N.I., and FISHER, P.B. (1995). Subtraction hybridization identifies a novel melanoma dif-

ferentiation associated gene, *mda-7*, modulated during human melanoma differentiation, growth and progression. Oncogene **11,** 2477–2486.

JIANG, H., SU, Z.Z., LIN, J.J., GOLDSTEIN, N. I., YOUNG, C.S., and FISHER, P.B. (1996). The melanoma differentiation associated gene *mda-7* suppresses cancer cell growth. Proc. Natl. Acad. Sci. USA **93,** 9160–9165.

KAWABE, S., NISHIKAWA, T., MUNSHI, A., ROTH, J.A., CHADA, S., and MEYN, R.E. (2002). Adenovirus-mediated mda-7 gene expression radiosensitizes non-small cell lung cancer cells via TP53-independent mechanisms. Mol. Ther. **6,** 637–644.

LEBEDEVA, I.V., SU, Z.Z., CHANG, Y., KITADA, S., REED, J.C., and FISHER, P.B. (2002). The cancer growth suppressing gene mda-7 induces apoptosis selectively in melanoma cells. Oncogene **21,** 708–718.

MADIREDDI, M.T., SU, Z.Z., YOUNG, C.S., GOLDSTEIN, N.I., and FISHER, P.B. (2000). *mda-7*, a novel melanoma differentiation associated gene with promise for cancer gene therapy. Adv. Exp. Med. Biol. **465,** 239–261.

MHASHILKAR, A.M., SCHROCK, R.D., HINDI, M., LIAO, J., SIEGER, K., KOUROUMA, F., ZOU-YANG, X.H., ONISHI, E., TAKH, O., VEDVICK, T.S., *et al.* (2001). Melanoma-differentiation associated gene-7 (*mda-7*): A novel anti-tumor gene for cancer gene therapy. Mol. Med. **7,** 271–282.

MHASHILKAR, A.M., STEWART, A.L., SIEGER, K., YANG, H.Y., KHIMANI, A.H., ITO, I., SAITO, Y., HUNT, K.K., GRIMM, E.A., ROTH, J.A., *et al.* (2003). MDA-7 negatively regulates the β-catenin and PI3K signaling pathways in breast and lung tumor cells. Mol. Ther. **8,** 207–219.

NISHIKAWA, T., RAMESH, R., CHADA, S., and MEYN, R. (2003). Adenovirus mediated mda-7 gene therapy suppresses angiogenesis and sensitizes NSCLC xenograft tumors to radiation. Proc. Am. Assoc. Cancer Res. **44,** 331.

PATAER, A., VORBURGER, S.A., BARBER, G.N., CHADA, S., MAHSHILKAR, A.M., ZOU-YANG, H., STEWART, A.L., BALACHANDRAN S., ROTH, J.A., HUNT, K.K., *et al.* (2002). Adenoviral transfer of the melanoma differentiation-associated gene 7 (mda7) induces apoptosis of lung cancer cells via up-regulation of the double-stranded RNA-dependent protein kinase (PKR). Cancer Res. **62,** 2239–2243.

RAMESH, R., SAEKI, T., TEMPLETON, N.S., JI, L., STEPHENS, L.C., ITO, I., WILSON, D.R., WU, Z., BRANCH, C.D., MINNA, J.D., *et al.* (2001). Successful treatment of primary and disseminated human lung cancers by systemic delivery of tumor suppressor genes using an improved liposome vector. Mol. Ther. **3,** 337–350.

RAMESH, R., MHASHILKAR, A.M., TANAKA, F., SAITO, Y., BRANCH, C.D., SIEGER, K., MUMM, J.B., STEWART, A.L., BOQUIO, A., DUMOUTIER, L., *et al.* (2003). Melanoma differentiation-associated gene 7/Interleukin (IL)-24 is a novel ligand that regulates angiogenesis via the IL-22 receptor. Cancer Res. **63,** 5105–5113.

SAEKI, T., MHASHILKAR, A., CHADA, S., BRANCH, C., ROTH, J.A., and RAMESH, R. (2000). Tumor suppressive effects by adenovirus-mediated mda-7 gene transfer in non-small cell lung cancer in vitro. Gene Ther. **7,** 2051–2057.

SAEKI, T., MHASHILKAR, A., SWANSON, X., ZOU-YANG, X.H., SIEGER, K., KAWABE, S., BRANCH C.D., ZUMSTEIN, L., MEYN, R.E., ROTH J.A., *et al.* (2002). Inhibition of human lung cancer growth following adenovirus mediated mda-7 gene expression in vivo. Oncogene **21,** 4558–4566.

SAITO, Y., MHASHILKAR, A.M., ROTH, J.A., CHADA, S, and RAMESH, R., (2003). Selective induction of apoptosis of cell cycle arrest and apoptosis in human prostate cancer cells through adenoviral transfer of the melanoma differentiation associated 7 (mda 7) gene. Proc. Am. Assoc. Cancer Res. **44,** 247.

SARKAR, D., SU, Z.Z., LEBEDEVA, I.V., SAUANE, M., GOPALKRISHNAN, R.V., DENT, P., and FISHER, P.B. (2002a). *mda-7* (IL-24): Signaling and functional roles. Biotechniques **8,** 30–39.

SARKAR, D., SU, Z.Z., LEBEDEVA, I.V., SAUANE, M., GOPALKRISHNAN, R.V., VALERIE, K., DENT, P., and FISHER, P.B., (2002b). mda-7 (IL-24) mediates selective apoptosis in human melanoma cells by inducing the coordinated overexpression of the GADD family of genes by means of p38 MAPK. Proc. Natl. Acad. Sci. USA **99,** 10054–10059.

SCHAEFER, G., VENKATARAMAN, C., and SCHINDLER, U. (2001). Cutting edge: FISP (IL-4-induced secreted protein), a novel cytokine-like molecule secreted by Th2 cells. J. Immunol. **15,** 5859–5863.

SIEGER, K.A, MHASHILKAR, A.M., STEWART, A., SUTTON, R.B., STRUBE, R.W., CHEN, S.Y., PATAER, A., SWISHER, S.G., GRIMM, E.A., RAMESH, R., *et al.* (2004). The tumor suppressor activity of MDA/IL-24 protein is mediated by intracellular protein expression in NSCLC cells. Mol. Ther. **9,** 355–367.

SU, Z.Z., MADIREDDI, M.T., LIN, J.J., YOUNG, C.S., KITADA, S., REED, J.C., GOLDSTEIN, N.I., and FISHER, P.B., (1998). The cancer growth suppressor gene *mda-7* selectively induces apoptosis in human breast cancer cells and inhibits tumor growth in nude mice. Proc. Natl. Acad. Sci. USA **95,** 14400–14405.

TEMPLETON, N.S., LASIC D.D., FREDERICK P.M., STREY, H.H., ROBERTS, D.D., and PAVLAKIS, G.N., (1997). Improved DNA:liposome complexes for increased systemic delivery and gene expression. Nat. Biotechnol. **15,** 647–652.

VARNAVSKI, A.N., ZHANG, Y., SCHNELL, M., TAZELAAR, J., LOUBOUTIN, J.P., YU., Q.C., BAGG, A., GAO, G.P., and WILSON, J.M., (2002). Preexisting immunity to adenovirus in rhesus monkeys fails to prevent vector-induced toxicity. J. Virol. **76,** 5711–5719.

VLACHAKI, M.T., HERNANDEZ-GARCIA, A., ITTMANN, M., CHHIKARA, M., AGUILAR, L.K., ZHU, X., TEH, B.S., BUTLER, E.B., WOO, S., THOMPSON, T.C., *et al.* (2002). Impact of preimmunization on adenoviral vector expression and toxicity in a subcutaneous mouse cancer model. Mol. Ther. **6,** 342–348.

YACOUB, A., MITCHELL C., BRANNON, J., ROSENBERG, E., QIAO, L., MCKINSTRY, R., LINEHAN, W.M., SU, Z.S., SARKAR, D., LEBEDEVA, I.V., *et al.* (2003a). MDA-7 (interleukin-24) inhibits the proliferation of renal carcinoma cells and interacts with free radicals to promote cell death and loss of reproductive capacity. Mol. Cancer Ther. **2,** 623–632.

YACOUB, A., MITCHELL C., LISTER, A., LEBEDEVA, I.V., SARKAR, D., SU, Z.Z., SIGMON, C., McKINSTRY, R., RAMAKRISHNAN, V., QIAO, L., *et al.* (2003b). Melanoma differentiation-associated 7 (interleukin 24) inhibits growth and enhances radiosensitivity of glioma cells in vitro and in vivo. Clin. Cancer Res. **9,** 3272–3281.

Address reprint requests to:
Rajagopal Ramesh, Ph.D.
Department of Thoracic and Cardiovascular Surgery
Unit 445
The University of Texas M.D. Anderson Cancer Center
1515 Holcombe Blvd.
Houston, TX 77030

E-mail: rramesh@mdanderson.org

Received for publication May 2, 2004; received in revised form July 9, 2004; accepted July 30, 2004.

doi:10.1016/j.ymthe.2004.09.021

Intratumoral Injection of INGN 241, a Nonreplicating Adenovector Expressing the Melanoma-Differentiation Associated Gene-7 (*mda-7*/IL24): Biologic Outcome in Advanced Cancer Patients

Alex W. Tong,[1,2,*] John Nemunaitis,[2] Dan Su,[1] Yuan Zhang,[1] Casey Cunningham,[2] Neil Senzer,[1,2] George Netto,[1] Dawn Rich,[2] Abner Mhashilkar,[3] Karen Parker,[3] Keith Coffee,[3] Rajagopal Ramesh,[4] and Suhendan Ekmekcioglu[5] Elizabeth A. Grimm[5] Jill van Wart Hood[3] James Merritt[3] Sunil Chada[3,5,†]

[1]*Baylor Sammons Cancer Center, Baylor University Medical Center, Dallas, TX 75246, USA*
[2]*US Oncology, 3535 Worth Street, Dallas, TX 75246, USA*
[3]*Introgen Therapeutics, Inc., Houston, TX 77030, USA*
[4]*Department of Thoracic and Cardiovascular Surgery and*
[5]*Department of Experimental Therapeutics, University of Texas M. D. Anderson Cancer Center, Houston, TX 77030, USA*

**To whom correspondence and reprint requests should be addressed at the Cancer Immunology Research Laboratory, Sammons Cancer Center, Baylor University Medical Center, 3500 Gaston Avenue, Dallas, TX 75246, USA.*

† To whom correspondence and reprint requests should be addressed at Introgen Therapeutics, Inc., Houston, TX 77030, USA.

Available online 5 November 2004

The *mda-7* gene (approved gene symbol IL24) is a novel tumor suppressor gene with tumor-apoptotic and immune-activating properties. We completed a Phase I dose-escalation clinical trial, in which a nonreplicating adenoviral construct expressing the *mda-7* transgene (INGN 241; Ad-mda7) was administered intratumorally to 22 patients with advanced cancer. Excised tumors were evaluated for vector-specific DNA and RNA, transgenic MDA-7 expression, and biological effects. Successful gene transfer as assessed by DNA- and RT-PCR was demonstrated in 100% of patients evaluated. DNA analyses demonstrated a dose-dependent penetration of INGN 241 (up to 4×10^8 copies/μg DNA at the 2×10^{12} vp dose). A parallel distribution of vector DNA, vector RNA, MDA-7 protein expression, and apoptosis induction was observed in all tumors, with signals decreasing with distance away from the injection site. Additional evidence for bioactivity of INGN 241 was illustrated via regulation of the MDA-7 target genes β-catenin, iNOS, and CD31. Transient increases (up to 20-fold) of serum IL-6, IL-10, and TNF-α were observed. Significantly higher elevations of IL-6 and TNF-α were observed in patients who responded clinically to INGN 241. Patients also showed marked increases of $CD3^+CD8^+$ T cells posttreatment, suggesting that INGN 241 increased systemic T_H1 cytokine production and mobilized $CD8^+$ T cells. Intratumoral delivery of INGN 241 induced apoptosis in a large volume of tumor and elicited tumor-regulatory and immune-activating events that are consistent with the preclinical features of MDA-7/IL-24.

INTRODUCTION

The melanoma differentiation associated gene-7 (*mda-7*; approved gene symbol IL24) was identified as one of several genes that were up-regulated during terminal differentiation of melanoma cells [1]. Subsequent gene transfer studies using plasmid-based or adenoviral vector-mediated delivery of *mda-7* (Ad-mda7) confirmed that *de novo* MDA-7 protein expression reduced growth and colony formation in a variety of human cancer models, including breast, lung, colon, and prostate carcinomas, but not normal cells [1–8]. Ad-mda7 selectively suppressed tumor cell growth via G2/M cell cycle blockade and apoptosis induction [2–8]. Tumor-selective apoptosis correlated with the up-regulation of BAX and caspase-3 cleavage [2–4] but was independent of JAK/STAT tyrosine kinases or p53/Rb status [2,4,7].

MDA-7 was recently designated as interleukin-24 (IL-24) based on limited sequence homology with IL-10, presence of the *mda-7*/IL24 gene in the IL-10 family cluster at 1q32, and expression in leukocytes [9,16]. Recombinant MDA-7 protein treatment of human peripheral blood mononuclear cells induced high levels of IL-6, TNF-α,

1525-0016/$30.00

and IFN-γ and low levels of IL-12 and GM-CSF, suggesting T_H1 cytokine-like activity for this molecule [9]. Additional anti-tumor effects have been demonstrated in Ad-mda7-infected tumor models, including the inhibition of cell migration and invasion, down-regulation of metalloproteases, and up-regulation of the E-cadherin–β-catenin adhesion complex [11,12]. Ad-mda7 treatment of non-small-cell lung cancer xenografts inhibited angiogenesis by reducing tumor microvessel density and down-regulating VEGF and TGF-β [5]. Anti-angiogenesis was mediated by bystander activity of secreted MDA-7 protein acting via the IL-22 receptor on endothelial cells [13].

In view of the direct tumor growth inhibitory effect of *mda-7* as well as its bystander features, we reviewed laboratory findings from a recently completed open-label, Phase I, dose-escalation trial on 22 advanced cancer patients who received intratumoral injection of INGN 241 [14]. INGN 241 is a nonreplicating adenovirus vector carrying the *mda-7* transgene [2]. Patients received single or repeated intratumoral injections of 2×10^{10} to 2×10^{12} viral particles (vp). Treatment was generally well tolerated, and durable clinical responses were observed in a subset of patients who received multiple intratumoral injections [14]. It was shown that intratumoral INGN 241 was associated with high levels of MDA-7 expression, which correlated with proapoptotic activity. After a single administration, MDA-7 transgenic protein and apoptosis induction were observed more than 3 cm from the injection site [14]. We now further demonstrate that the clinical activities of INGN 241 encompassed apoptotic, anti-proto-oncogene signaling and systemic immune activation. These results indicate that INGN 241 holds promise as an experimental therapeutic that can generate direct tumor growth inhibition and bystander anti-tumor effects.

RESULTS

Transgene Expression Following Intratumoral Injection With INGN 241

We stratified the patients into eight cohorts according to viral dose (2×10^{10} to 2×10^{12} vp), time of posttreatment biopsy (24 h to 30 days), and treatment mode (single dose, divided dose, or multiple injections) as described under Materials and Methods (Table 1). To understand better the safety and efficacy of INGN 241 treatment, we performed cell and molecular analyses to characterize transgene expression and pharmacokinetics, biologic activity, and immune response. Prior to injection, we mixed the INGN 241 vector with Lymphazurin (Isosulfan blue), a dye commonly used in lymph node mapping. Previous studies demonstrated that dye addition does not inhibit adenoviral transduction *in vitro* or *in vivo* (unpublished data). The dye signal persists in tumors for multiple days and facilitates identification of injection site in resected tumors [14]. Upon resection, we bisected the tumors along the injection site and sectioned each hemi-tumor to give three to five sections. We froze sections from one-half of the tumor immediately in liquid nitrogen for analysis by quantitative DNA PCR and RT-PCR; we fixed, paraffin embedded, and evaluated by immunohistochemistry (IHC) sections from the other half-tumor.

For patients entered into cohorts 1–6, we resected the vector-treated tumor at 24–96 h postinjection (lesion diameter varied from 1.8 to 8.1 cm). We evaluated serial sections for vector penetration and biologic outcome. We obtained pretreatment biopsies from 9 of 10 patients in cohorts 1–6: all samples were MDA-7 negative by IHC. We observed strong MDA-7 staining in treated lesions: a representative example of transgenic MDA-7 protein expression is illustrated in Fig. 1A. Staining patterns consisted of intense focal areas surrounded by more diffuse staining: this punctate pattern of immunostaining is consistent with transduced cells expressing high levels of intracellular and secreted MDA-7. One hundred percent of INGN 241-injected lesions showed high levels of MDA-7 immunoreactivity in the center (injection site). Signal intensity was reduced at the distal sections in each tumor, although 7 of 10 injected lesions still showed MDA-7 immunoreactivity (Fig. 1B), at distances up to 3 cm from the injection site. At 24 h postinjection, the mean proportion of tumor cells expressing MDA-7 protein ranged from 20% in cohort 1 patients, who received 2×10^{10} vp,

TABLE 1: Patient cohorts and treatment profile

Cohort (No. of pts)	No. of viral particles	Biopsy time	Diagnosis of evaluable patients[a] (No. tested)
1 (1)	2×10^{10}	+24 h	BrCa (1)
2 (1)	2×10^{11}	+24 h	CoCa (1)
3 (3)	2×10^{12}	+24 h	SCCHN (1), Mel (1), LCL (1)
4 (3)	2×10^{12}	+48 h	BrCa (1), AdrCa (1), Hep (1)
5 (3)	2×10^{12}	+96 h	BrCa (1), Mel (1), Mel (1)
6 (1)	2×10^{12}, divided dose	+48 h	BrCa (1)
7 (5)	2×10^{12}	Day 30	TCC (1), Mel (1), CoCa (1), SCCHN (2)
8 (5)	2×10^{12}; twice weekly ×3	Day 30	Mel (3), SCCHN (2)

[a] BrCa, breast carcinoma; CoCa, colon carcinoma; SCCHN, squamous cell carcinoma of the head and neck; Mel, melanoma; LCL, large cell lymphoma; AdrCa, adrenal carcinoma; Hep, hepatoma; TCC, transitional cell carcinoma.

doi:10.1016/j.ymthe.2004.09.021

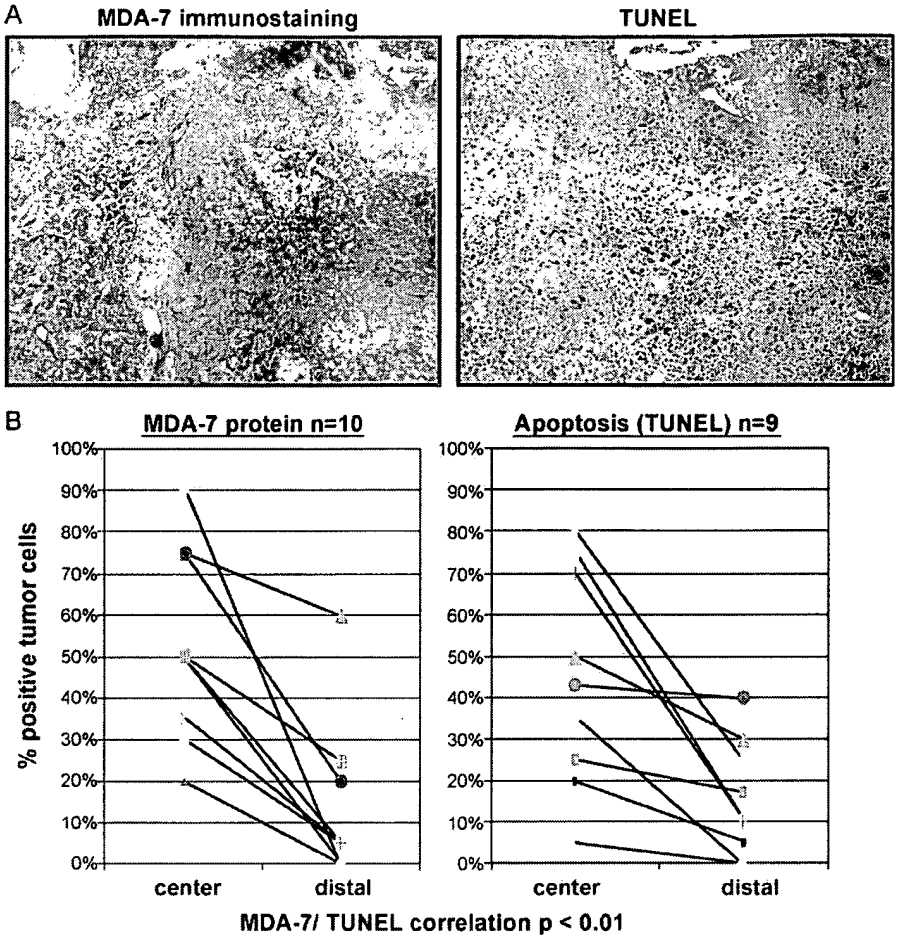

FIG. 1. Intratumoral expression of MDA-7 colocalizes with apoptotic regions. (A) Apoptosis induction corresponds geographically to regions of high MDA-7 immunostaining. Representative serial sections taken 12 mm from the injection site from patient 3 were stained for MDA-7 expression and apoptosis. Note the intense foci of MDA-7 staining within cells as well as diffuse signal between cells. TUNEL signals correspond to regions of intense MDA-7 staining. (B) INGN 241 injection elicits high level MDA-7 expression and apoptosis induction. Samples from injection site (center) and distal portion of tumors were evaluated for MDA-7 immunostaining (n = 10) and apoptosis via TUNEL staining (n = 9). Pretreatment MDA-7 staining was uniformly negative, whereas TUNEL signal averaged 5.6% in pretreatment samples. Average MDA-7 staining was 52% in the central region and 14% in the distal region of tumors. Apoptosis signals averaged 45% in the central region and 15% in the distal region. MDA-7 expression correlates significantly with TUNEL reactivity ($P < 0.01$; linear regression analysis) (C) High levels of transgene expression and apoptosis are transient. Pretreatment and injection site sections were analyzed for MDA-7 immunostaining or apoptosis by TUNEL assay and median values plotted. MDA-7 immunostaining correlated with TUNEL reactivity and peaked at day 4 postinjection. Day 1, n = 5 patients; day 2, n = 3; day 4, n = 2; day 30, n = 7. By day 30, MDA-7 staining and apoptosis were undetectable.

to a mean of 53% in cohort 3 patients, who received 2×10^{12} vp. The majority (>85%) of MDA-7-immunostained cells exhibited malignant histological features: a few histocytic/reticuloendothelial cells/lymphocytes also showed positive staining.

Cohorts 3–5 received the same intratumoral viral dose (2×10^{12} vp). The injected tumors were biopsied at 24, 48, and 96 h, respectively. This limited analysis with two or three patients per time point nonetheless illustrated the sustained expression of the MDA-7 protein (Fig. 1C), in that we observed a median frequency of 70% transgene-positive tumor cells at 96 h postinjection. MDA-7 staining was not detected in samples obtained at 30 days (Fig. 1C). Quantitative DNA PCR (qPCR) analysis for vector genomes demonstrated a correspondingly high level of viral DNA (equivalent to 740–900 copies per cell)

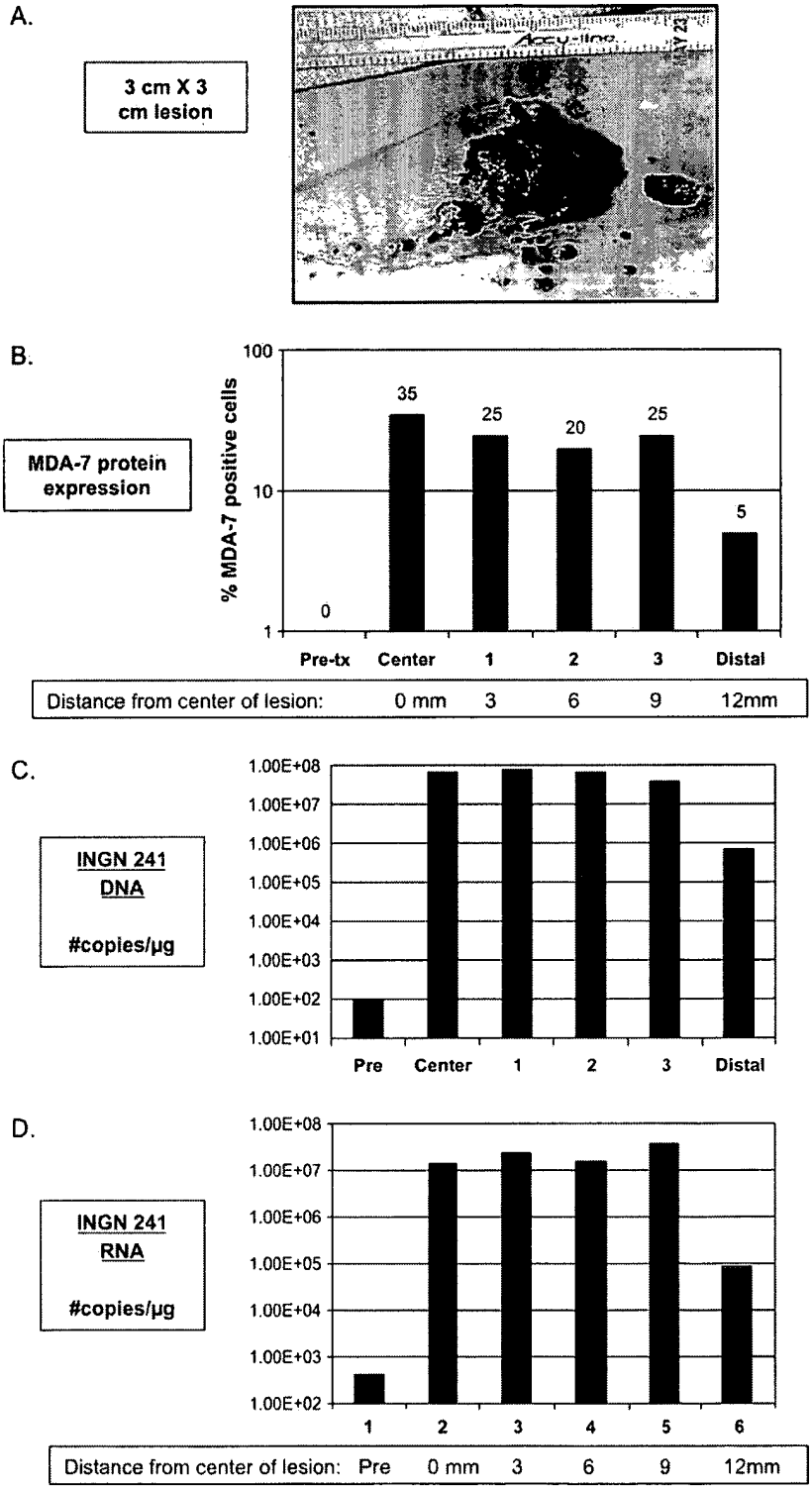

FIG. 2. Molecular analyses of vector distribution and expression in a melanoma patient. (A) Patient 4 (metastatic melanoma) was injected with 2×10^{12} vp INGN 241 and resected 24 h later. (B) Sections were immunostained for MDA-7 protein and percentage MDA-7-positive cells was quantified. Pretreatment sections were negative, whereas injection site showed 35% positive tumor cells. Percentage stained cells and their staining intensity decreased with distance from injection site. (C) DNA was isolated from pretreatment and posttreatment sections and subjected to quantitative PCR analysis. Data are shown as number of DNA copies of INGN 241 per microgram of tumor DNA. High levels of vector DNA are observed close to the injection site and fall with distance. (D) RNA was isolated from pretreatment and posttreatment sections and subjected to quantitative RT-PCR analysis. Data are shown as number of RNA copies of INGN 241 per microgram of tumor RNA. High levels of vector-specific RNA are observed close to the injection site and fall with distance. Note correpondence between vector nucleic acid and Mda-7 protein expression.

doi:10.1016/j.ymthe.2004.09.021

in the injected lesions at days 1 and 2, which markedly decreased at 4 days postinjection (1 copy/cell) and 30 days postinjection (0.04 copy/cell) [14]. RT-PCR analysis of biopsy sections at the point of injection verified the presence of the INGN 241 viral mRNA at approximately 1×10^7 copies/μg at day 1 (cohort 3), 1.2×10^6 copies/μg at day 2 (cohort 4), and 8×10^4 copies/μg at day 4 [14].

Tumor Apoptotic Activity Correlated with MDA-7 Penetration

We observed pronounced apoptotic activity in INGN 241-injected tumors that corresponded to areas of MDA-7 expression (Fig. 1A) in injected lesions resected after 24–96 h. Apoptotic signals were greatest in the high-dose group (2×10^{12} vp) and could still be detected in distal sections of the tumor in seven of nine evaluable patients (Fig. 1B). The low-dose tumors also exhibited apoptosis at the injection site, but signal at the periphery of these tumors did not differ from pretreatment samples. Similar to the MDA-7 distribution, apoptotic activity appeared to accumulate with time in patients who received INGN 241, with 36, 39, and 58% of total tumor cells revealing a positive TUNEL reaction at 24 ($n = 5$), 48 ($n = 5$), and 96 h ($n = 2$) postinjection (Fig. 1C). The frequency of apoptotic tumor cells displayed a similarly graded pattern, which correlated with MDA-7 expression (Fig. 1B; $P < 0.01$, $n = 9$). These findings indicate that INGN 241 expression contributed significantly to posttreatment tumor apoptosis. Consistent with the anti-tumor effect, Ki-67 staining (to assess tumor cell proliferation) was decreased after INGN 241 injection in six of nine (67%) evaluable tumors (not shown).

Molecular Markers of Vector Expression Correlate with Biological Activity

We evaluated serial tumor sections for vector-specific DNA, RNA, transgenic protein, and biological outcome. A representative panel of assays is shown in Fig. 2, which illustrates the correlation observed between vector nucleic acids and transgenic protein. In this metastatic melanoma (Fig. 2A), serial sections exhibited 35% MDA-7 immunostaining in the center of the tumor, decreasing to 5% in distal sections (≥12 mm from injection site) (Fig. 2B). The pretreatment lesion did not show detectable MDA-7 immunostaining. Vector DNA and RNA levels remained high for at least 9 mm from the injection site and then decreased beyond this point: samples taken at 12 mm showed greater than 95% reduction in signal (Figs. 2C and 2D).

MDA-7 has been shown to lower the expression of proto-oncogenes involved in β-catenin and PI3K signaling in human breast and lung cancer models [11,12] and to down-regulate the melanoma progression molecule iNOS (inducible nitric oxide synthase) in melanoma cell lines [15]. We carried out immunohistochemical evaluations to quantify β-catenin and iNOS expression in INGN 241-treated lesions. Four patients in cohorts 1–6 were diagnosed with metastatic breast cancer at the time of treatment. Their untreated tumors displayed a uniform, diffuse nuclear/cytoplasmic pattern of β-catenin expression. Three cases underwent a distinct redistribution of this protein to the plasma membrane posttreatment. While β-catenin redistribution was evident in other nonbreast tumors examined, the majority of these cases (six of eight tested) exhibited a significantly decreased level of β-catenin expression following intratumoral INGN 241 (Table 2 and Fig. 3). Evaluation of biopsy samples from a colon carcinoma patient showed high levels of β-catenin immunostaining in the nucleus and cytoplasm prior to treatment (Fig. 3A). After INGN 241 injection, levels of β-catenin expression were markedly diminished as shown in the posttreatment section (Fig. 3A). Distal sections showed levels of β-catenin comparable to those of the pretreatment samples and correlated with loss of MDA-7 immunostaining. The lower panel (Fig. 3B) shows immunostaining of a hepatoma lesion and provides additional support for an inverse correlation between β-catenin immunostaining and MDA-7 expression. Sections proximal to the injection site of this large lesion (8.1 × 11 cm) showed 50% MDA-7 immunostaining, whereas serial sections showed very weak β-catenin expression. In contrast, distal sections (>3 cm from injection site) have lost MDA-7 expression and show increased β-catenin reactivity.

iNOS has been reported as a promising prognostic marker for malignant melanoma [21] and recent studies have shown that Ad-mda7 and secreted MDA-7 protein

TABLE 2: β-Catenin expression in INGN 241-treated patient specimens

Cohort	Patient diagnosis	Effect of treatment on β-catenin expression	
		Redistribution to membrane	Decreased expression
1	BrCa	Yes	No
2	CoCa	[b]	Yes
3[a]	SCCHN	[b]	Yes
4	BrCa	Yes	No
	AdrCa	n/a	Yes
	Hep	Yes	n/a
5	BrCa	n/a	n/a
	Mel	No	Yes
	Mel	Yes	Yes
6	BrCa	Yes	Yes
No. positive/ No. evaluable		5/8	6/8

n/a, not analyzed.

[a] Patient 4 was not examined due to lack of specimen. Patient 5 was diagnosed with large cell lymphoma that did not express β-catenin.

[b] Qualitative differences that cannot be definitely identified as redistribution were observed.

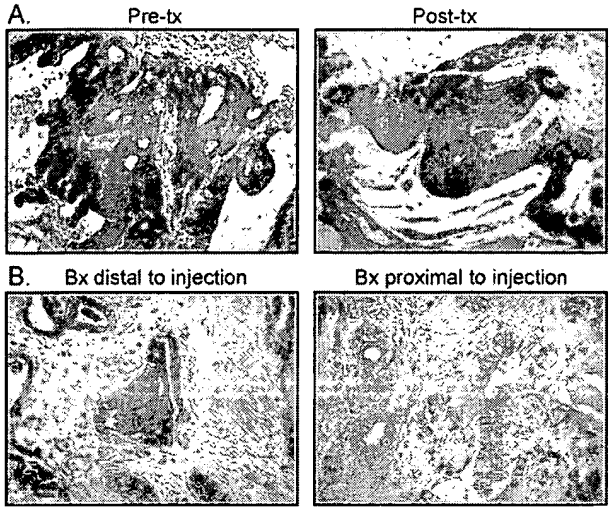

FIG. 3. β-Catenin expression is reduced after INGN 241 treatment. (A) Biopsy from patient with metastatic colon cancer—posttreatment sections show reduced β-catenin staining intensity compared to pretreatment sections. (B) Patient with hepatoma—sections close to injection site show reduced β-catenin staining intensity compared to samples distal to the injection site.

can down-regulate iNOS expression in melanoma tumor cells via regulation of interferon regulatory factor 1/2 signaling [15]. In two of three melanoma cases from cohorts 1–6, we observed strong decreases in iNOS expression after INGN 241 injection (Figs. 4A and 4B). Pretreatment biopsies indicated high levels of iNOS staining (Fig. 4A; red staining) and no MDA-7 staining. The center of the injected lesion showed complete loss of iNOS immunoreactivity and serial sections showed 35% MDA-7-positive cells. The distal region of the lesion (>1 cm from the injection site) showed weak iNOS immunostaining and 5% MDA-7 reactivity (Fig. 4A). A second melanoma showed high levels of iNOS expression in the pretreatment biopsy, whereas the center of the injected lesion showed marked reduction of iNOS expression (Fig. 4B) that correlated with high level staining of MDA-7. Loss of iNOS staining persisted to distal regions of tumor. *In toto*, four of nine cases of various solid tumor types showed a decrease in iNOS following INGN 241 treatment (data not shown).

Recent studies have demonstrated that Ad-mda7 inhibits primary endothelial cell differentiation and exhibits antiangiogenic activity [5]. Ad-mda7 significantly suppressed radiation-induced VEGF, bFGF, and IL-8 production in lung tumor xenografts [37]. Additional studies have shown that MDA-7 protein is responsible for the observed activity and is 50-fold more potent than endostatin or angiostatin [13,37,39]. MDA-7 regulates angiogenesis via interaction with a specific receptor, IL-22R1/IL-20R2 [13]. We evaluated CD31 immunostaining (as a marker for tumor vasculature) in cohort 7 tumors, which we resected 30 days after a single injection of INGN 241. Two patients did not have a pretreatment biopsy available; however, in the remaining three cases, an average of 28% reduction in CD31 staining was observed in the day 30 specimen compared to pretreatment.

INGN 241 DNA Intratumoral and Systemic Pharmacokinetics

We carried out intratumoral INGN 241 DNA pharmacokinetic analyses by quantifying vector DNA recovered

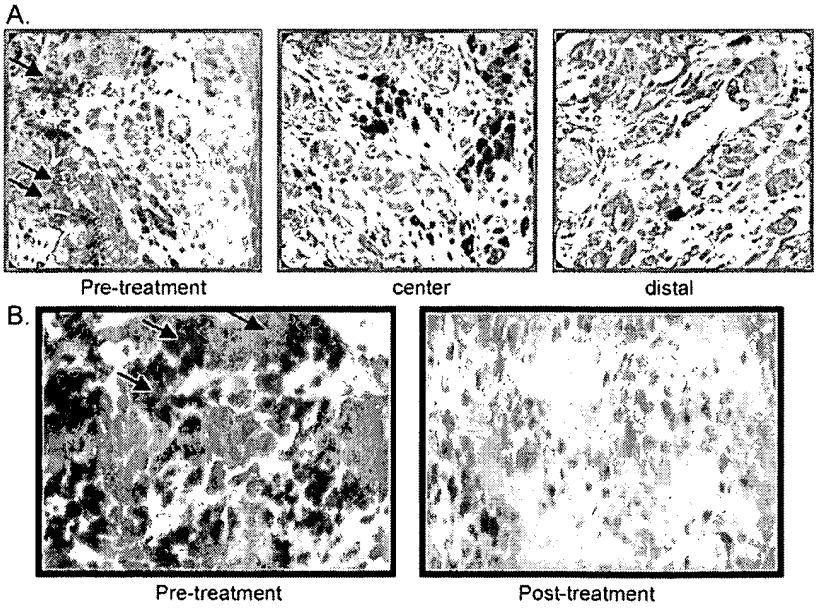

FIG. 4. INGN 241 injection causes loss of iNOS in melanoma patients. Patient sections were immunostained for iNOS expression. (A) Strong iNOS staining pretreatment in melanoma, whereas injection site (center) is negative for iNOS. A graded increase in iNOS was observed distal to the injection site, with highest levels at the tumor periphery (although still lower than pretreatment). iNOS signals are shown by red staining (arrows); note that the brown staining is due to melanin. (B) Pretreatment staining in melanoma shows strong iNOS staining (indicated by arrows), whereas posttreatment iNOS is reduced throughout the tumor.

doi:10.1016/j.ymthe.2004.09.021

from serial sections of injected tumors, with the assumption that recovered DNA was cell associated. The levels of vector-specific DNA at the injection site for patients 1–10 are shown in Fig. 5A. Pretreatment samples showed an average of 440 vector DNA copies/μg genomic DNA. All lesions sampled after INGN 241 injection showed elevated levels of vector DNA, demonstrating successful gene transfer in all injected lesions. DNA levels decreased with time: average DNA yields at the injection site were 2.2×10^8 DNA copies/μg genomic DNA at 24 h postinjection, 9.8×10^7 copies/μg at 48 h, and 1.2×10^5 copies/μg at 96 h. We compared the total number of vector DNA copies in the tumor with total vector injected to yield the percentage vector DNA recovered from tumor as a function of time (Fig. 5B). After 24 h, 11.7% of total input viral DNA remained in the injected tumor lesion, which was reduced to 1.7 and 0.03% of input load at days 2 and 4. By 30 days postinjection, only 0.0001% of injected vector was recovered from the tumor (Fig. 5B).

We evaluated the presence of circulating INGN 241 vector in patient plasma using quantitative DNA PCR. INGN 241 vector DNA was transiently detected in plasma in both a dose- and a time-dependent manner (Fig. 6A). INGN 241 was detectable in plasma within 30 min after intratumoral injection in all patients analyzed. In cohort 1 and 2 patients, plasma vector was undetectable by 24 h, whereas higher doses of vector were not cleared until 24–72 h postinjection. In all patients evaluated (n = 9), circulating vector was no longer detectable after 72 h (Fig. 6A). The average amount of injected vector detected in the circulation at 30 min constituted approximately 3% of the intratumorally injected dose (Fig. 6B). Systemic vector DNA levels fell exponentially, with only 0.0025% of injected vector remaining by 24 h after injection. From these data, we calculate the half-life of INGN 241 in systemic circulation to be approximately 11 min.

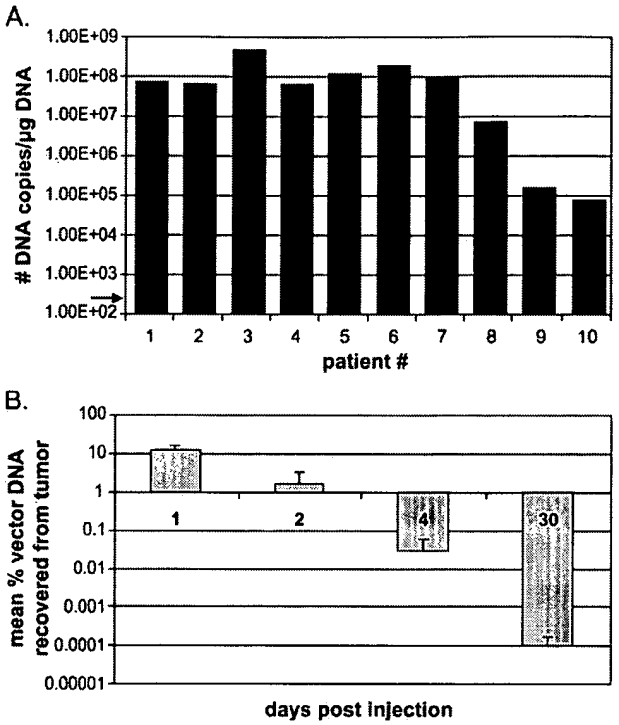

FIG. 5. Intratumoral INGN 241 DNA pharmacokinetics. (A) INGN 241 vector DNA decreases with time. DNA was isolated from the center section of lesions from patients 1–10 and analyzed for INGN 241-specific DNA. Pretreatment samples gave an average signal of 4.4×10^2 DNA copies per microgram DNA (n = 8; arrow). Patients 1–5 were resected at 24 h; patients 6–8 were resected at 48 h, and patients 9 and 10 were resected at 96 h postinjection. Lower limit of detection of vector DNA in tumor sections is 100 copies/μg. (B) Intratumoral decay of INGN 241 vector DNA. Tumor sections were evaluated for presence of vector DNA by quantitative DNA PCR and total vector-specific DNA was quantitated for each tumor. The intratumoral vector DNA burden was compared to the input vector injected. Data are plotted as mean % vector DNA recovered over time. Samples were evaluated for day 1 (n = 4 tumors), day 2 (n = 3 tumors), day 4 (n = 2), and day 30 (n = 4). Average vector recovery at day 1 was 12% (range 23–7%). By day 30, only 0.0009% of input vector was recovered. The x axis indicates time of tumor resection. Data are shown as means + SEM.

Immune Activation by INGN 241

To identify systemic immune activation events following intratumoral INGN 241, we quantified serum cytokines at various times after INGN 241 injection. The majority of patients had significantly elevated levels of serum IL-6 (19 of 22 patients), IL-10 (19/22), and TNF-α (12/22) following INGN 241 injection, with smaller numbers of patients exhibiting increased levels of IFN-γ, GM-CSF, and IL-2 that were ≥50% higher than baseline level within 8 days postinjection. Posttreatment levels of IL-6, IL-10, and IFN-γ constituted up to 20-fold higher than pretreatment level. The initial peak responses of IL-6 and TNF-α occurred at 6 h posttreatment for most patients, whereas maximal IFN-γ and IL-10 responses occurred at day 2 postinjection (Fig. 7A). In patients treated with a single injection of INGN 241 (cohorts 1–7), a second peak of IL-6 was evident on day 4. Circulating levels of TNF-α, IFN-γ, and IL-10 showed a second peak at day 8 (data not shown). Serum cytokine levels returned to baseline by days 15–30 after INGN 241 injection.

We also evaluated tumor RNA samples via RT-PCR for modulation of intratumoral cytokine mRNAs. Due to material limitations, only a subset of tumor RNAs was available for analysis for expression of IL-6, IL-10, and IFN-γ mRNAs. No cytokine mRNA changes were noted in tumors injected with low dose of vector (i.e., cohort 1 or 2). However, four of five tumors from high-dose patients showed elevated levels of IL-6 and IL-10 mRNA, whereas three tumors showed elevated IFN-γ mRNA. Cytokine mRNA increases were observed in two patients with melanoma, one each lymphoma and hepatoma.

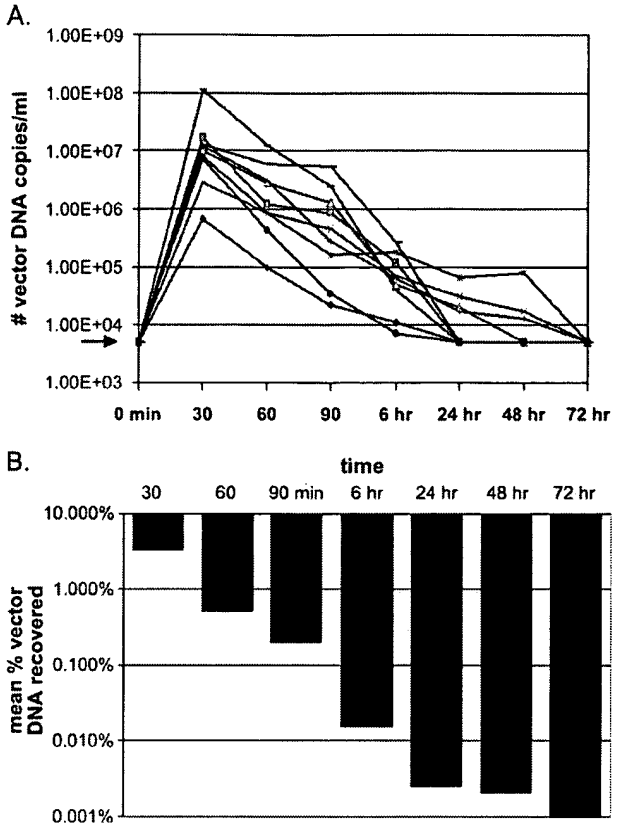

FIG. 6. Systemic INGN 241 pharmacokinetics. (A) INGN 241 circulates transiently. Plasma was sampled at the indicated times and analyzed for vector DNA using quantitative DNA PCR. Individual patient samples are shown (n = 9). Lower limit of detection of vector DNA in plasma is 5000 copies/ml and is indicated by the arrow. (B) INGN vector decay in plasma. Plasma samples were evaluated for presence of vector DNA by quantitative DNA PCR and total vector-specific DNA was quantitated at each time point. The plasma vector DNA burden was compared to the input vector injected. Data are plotted as mean % vector DNA recovered over time. Average vector recovery at 30 min was 3.3% of input vector. By 72 h, no signals over background were detected. n = 9 patients.

For cohort 8 patients, who received biweekly repeat injections, cytokine responses did not appear to be significantly heightened compared with time of initial exposure, with the exception of IL-10, for which reinjection elicited a greater than or equal to twofold elevated response compared to initial injection in three of five patients (data not shown). Two patients (of five completing one cycle of treatment) in cohort 8 demonstrated objective clinical responses following repeated injections with INGN 241 [14]. Both patients exhibited marked elevations in IL-6 (peak increases of 134–3085% over baseline), IL-10 (2519–3079%), and TNF-α (95–115%). However, these increases did not differ markedly from those of patients exhibiting stable disease in the same cohort.

For patients who received 2×10^{11} or 2×10^{12} vp INGN 241, 10 of 21 exhibited an increase in the posttreatment frequency of $CD3^+CD8^+$ peripheral blood T cells. Despite the interpatient variation of the frequency distribution of $CD8^+$ T cells before treatment, there was a significant elevation in percentage $CD8^+$ T cells ($P < 0.03$, $df = 40$) at day 15 postinjection (from mean pretreatment level of 31 ± 2.4 to 38 ± 2.6% at day 15) (Fig. 7B). This increase in $CD3^+CD8^+$ T cell frequency was confirmed by the corresponding increase in absolute $CD8^+$ cell numbers ($P = 0.02$, $df = 40$ at day 15) and was similarly distributed among cohorts receiving single or multiple INGN 241 injections. We also calculated the ratio of CD4:CD8 cells at each analytic time point. As a whole, pretreatment CD4:CD8 ratios for the patient cohorts were markedly below the normal value of 2, reflecting the lower than normal frequency of $CD4^+$ T cells that we previously observed in advanced cancer patients [31]. In this study, the increase in $CD8^+$ T cells paralleled significantly the reduced CD4:CD8 ratio posttreatment (from 1.2 ± 0.1% at day 0 to 0.9 ± 0.07% at day 15; $P < 0.03$) (Fig. 7B).

We also evaluated patient plasma samples for induction of anti-Ad antibody responses. Fourteen patients in cohorts 1–7 were tested for the presence of anti-adenoviral antibodies. All had elevated antibody titers posttreatment that increased with time, with a median titer that was 64-fold higher than pretreatment level at day 15 postinjection (Fig. 7C). All patients showed increased anti-Ad antibody responses 8 days after a single INGN 241 injection, and the majority showed further elevations at day 15.

DISCUSSION

mda-7 was identified as a differentiation-induced gene; however, its anti-tumor properties were quickly realized [1]. The apoptosis-inducing effect of *mda-7* gene transfer was initially demonstrated in breast tumor cell lines [17]. Subsequently, a number of growth regulatory pathways have been identified after Ad-mda7 transduction into tumor cells: these include cell cycle arrest, changes in the ratio of proapoptotic (BAX, BAK) to antiapoptotic (BCL-2, BCL-XL) proteins, increased expression of the Ser/Thr kinase PKR and GADD (growth arrest and DNA damage) families of genes, down-regulation of oncogenic and up-regulation of tumor suppressor pathways, and inhibition of invasion/metastasis [1–8,10–12,35]. Ad-mda7 has shown potent anti-tumor activity in many different tumor types, including melanoma, glioblastoma multiforme, osteosarcoma, and carcinomas of the breast, cervix, kidney, colon, lung, nasopharynx, and prostate. Importantly, these anti-tumor effects are not evident in normal cells [33,34]. As a supplement to apoptosis induction by Ad-mda7, additional anti-tumor properties have been identified. These include inhibition of tumor cell invasion and metastasis [11,12], potent antiangiogenic effects mediated by MDA-7 protein [5,13,37,39], immunomodulation [9,33] and direct bystander cytotoxicity [40, manu-

doi:10.1016/j.ymthe.2004.09.021

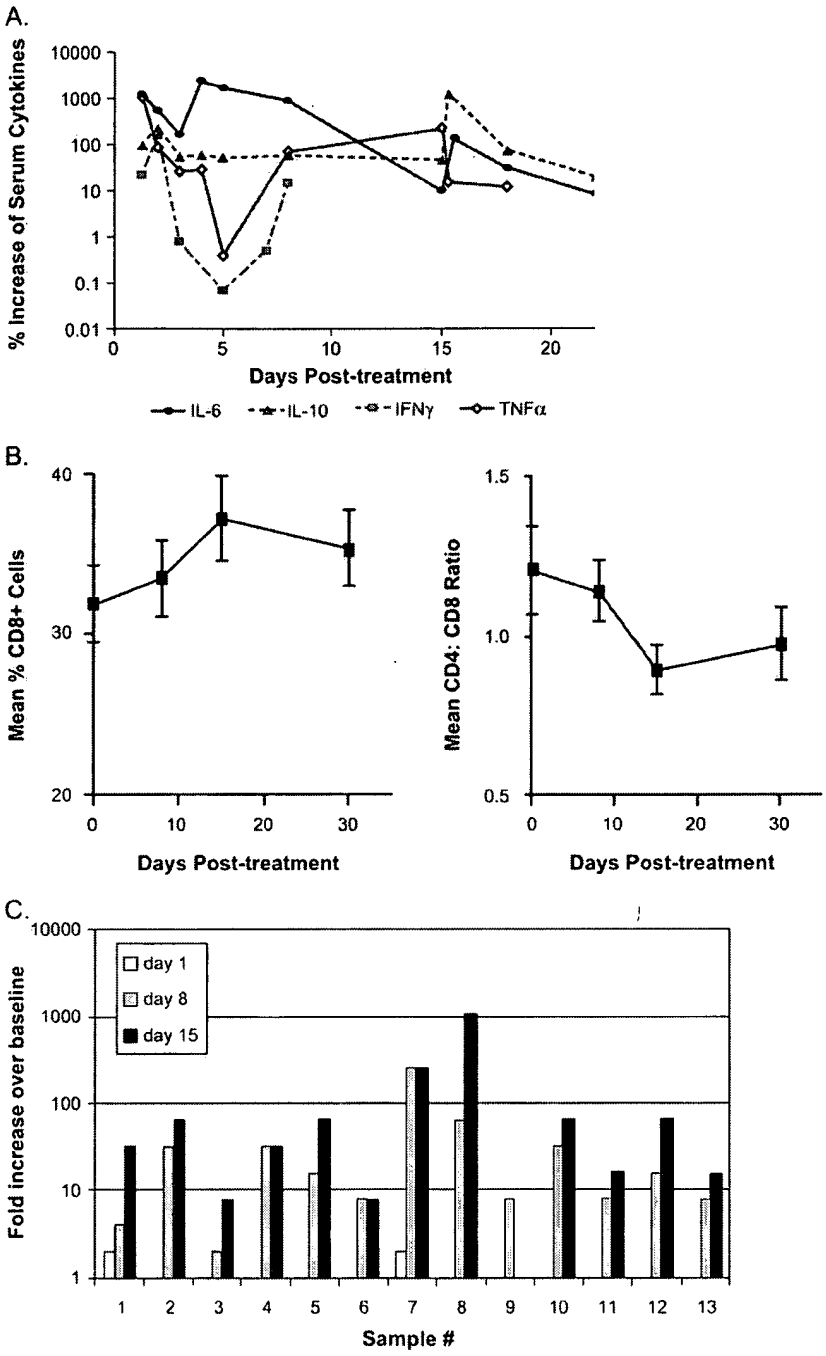

FIG. 7. Pharmacokinetics of serum cytokine response. (A) INGN 241 injection induces cytokine activation. Serum cytokine level of individual patients was determined by ELISA and compared with the baseline value to establish the % increase at the indicated time point postinjection. Value represents mean % increase for the 22 patients who completed the trial. Data for days 15–18 were derived only from patients in cohort 8, who received a second INGN 241 injection on day 15. (B) Effects of Ad-mda7 intratumoral injection on the frequency of peripheral blood $CD8^+$ T cells. The frequency distribution of peripheral blood $CD3^+CD8^+$ mononuclear cells was determined by two-color immunofluorescence flow cytometric analysis. Values represent mean frequency (±SEM) for all patients tested at the indicated time points. The patients' relative frequency of $CD3^+CD4^+$ and $CD3^+CD8^+$ T cells was represented as a CD4:CD8 ratio. Mean ratio (±SEM) for all patients tested at each time point is shown. Significance levels were evaluated using Student's *t* test. (C) Increase in anti-adenovirus antibody responses after INGN 241 injection. Anti-adenoviral responses were measured in patient serum prior to and after INGN 241 injection. The fold increase in anti-Ad vector titer was compared to pretreatment anti-Ad levels (baseline values set at 1).

script in preparation]. The broad spectrum and tumor-selective proapoptotic activity of Ad-mda7, coupled with the potential for bystander activities mediated by tumoricidal, antiangiogenic, and/or immunostimulatory mechanisms, suggests that *mda-7* gene drugs may provide additional molecularly targeted weapons in combating cancer [33,34].

In this study, we documented successful gene transfer in 100% of patients evaluated (Fig. 5A and [14]); this resulted in high levels of transgenic MDA-7 and apoptosis in all patients (Figs. 1A and 1B). Delivery of INGN 241 resulted in a consistent and pronounced apoptotic effect for at least 96 h postinjection for patients who received intratumoral injections of 2×10^{10} to 2×10^{12} vp of

INGN 241 (Fig. 1C). Close correlations were observed between vector-specific DNA and RNA levels and the resulting biologic sequelae of MDA-7 expression, namely apoptosis induction and regulation of downstream target molecules. The level of apoptosis observed in this study exceeded findings from other clinical gene delivery studies [19,20]. The enhanced proapoptotic efficacy, together with its direct correlation with MDA-7 penetration and expression over time, provides indirect evidence that MDA-7 expression contributed to the tumor apoptotic process that appeared to be independent of tumor histotype. It is notable that of the seven distinct tumor types in cohorts 1–6 evaluated (Table 1), all showed high levels of transgenic MDA-7 expression and apoptosis induction. This result is consistent with preclinical studies demonstrating apoptosis induction in a wide variety of tumor types, independent of histotype.

Preclinical studies in human breast and lung tumor models showed that MDA-7 induced tumor growth inhibition and collaterally altered the expression of tumor suppressor genes (E-cadherin, APC, GSK-3β, PTEN) and proto-oncogenes involved in β-catenin and PI3K signaling [11,12,32]. While the requirements for breast and lung cancer killing differed with respect to MAPK and MEK1/2 signaling, both cell types manifested a redistribution of cellular β-catenin from the nucleus to the plasma membrane, resulting in reduced TCF/LEF transcriptional activity. Evaluation of additional cancer cell lines shows that MDA-7 expression can also induce loss of steady-state β-catenin expression [32]. The majority of breast cancer patients who received intratumoral INGN 241 displayed a redistribution of β-catenin to the plasma membrane in their injected tumors (Table 2 and Fig. 3). Interestingly, a decreased expression of this transcription factor was evident in most other INGN 241-treated lesions. However, further studies are needed to define the differing outcomes of *mda-7* transgene expression on β-catenin transcription and protein localization in various tumor histologic types.

By comparison, our evaluations revealed a decreased level of iNOS expression in only four of nine patients tested, including two of three melanoma lesions tested. Constitutive iNOS expression has been described as a poor prognostic marker in melanoma, and iNOS expression is reflective of disease progression [21] and inversely correlated with MDA-7 in primary and metastatic melanomas [15]. Further, iNOS expression was down-regulated in a dose-dependent fashion after treatment with Ad-mda7 in melanoma cell lines. Our clinical findings in a small group of melanoma samples support the preclinical data indicating down-regulation of iNOS by MDA-7, but this effect may not extend broadly to other tumor types.

Based on limited primary sequence identity and predicted structural homology to IL-10, MDA-7 has been designated as IL-24 [9,22]. Soluble MDA-7/IL-24 induced the secretion of high levels of IL-6, TNF-α, and IFN-γ, together with low levels of IL-1β, IL-12, and GM-CSF from human peripheral blood lymphocytes [9]. These findings support the premise that MDA-7/IL-24, like other novel cytokines of the IL-10 family (IL-19, -20, -22, -26), may be involved in the regulation of inflammation and immune responses.

We observed a similar serum cytokine profile of pronounced elevations of IL-6, TNF-α, and IFN-γ in most patients who received intratumoral INGN 241. GM-CSF was also elevated in a small proportion of patients. The release and/or production of proinflammatory cytokines, including IL-6, TNF-α, IL-8, GM-CSF, and MIP-2, has also been detected by us and others following *intravascular* administration of the selective replicative, oncolytic adenovirus ONYX 015 [23,24]. Despite introduction by the intratumoral route, INGN 241 elicited a more sustained and heightened IL-6 response that peaked at day 4, whereas IL-10 responses were markedly decreased. According to viral DNA decay analysis, circulating INGN 241 concentration was markedly lower than that of ONYX 015 within the same time frame by at least 2 orders of magnitude and presumably would generate a correspondingly lower virus-dependent immune activation. Hence the sustained and heightened IL-6 and TNF-α response that far exceeded the levels induced by a *replicating* adenovirus is consistent with an activating role by the soluble mediator MDA-7/IL-24. Although there is limited information regarding the proinflammatory features of intratumoral adenovector injection, we favor the explanation that the observed immune activation events are manifestations by both the adenovirus backbone and the MDA-7 protein. A significant increase in the $CD3^+CD8^+$ T cells in the majority of patient cohorts at day 15 posttreatment is further indication of the delayed immune activation mediated by INGN 241. Increases in circulating $CD3^+CD8^+$ T cells have not been described in other clinical trials utilizing adenovectors. However, further analyses are needed to establish the anti-tumor activity of the elevated $CD8^+$ T cell subset that is commonly associated with cytotoxic effector function.

Intratumoral injection of INGN 241 at 2×10^{11} or 2×10^{12} vp resulted in sustained expression of the *mda-7* transgene for at least 96 h. While intratumoral viral DNA remained elevated compared with pretreatment level at day 30, MDA-7 transgenic protein and TUNEL reactivity were no longer detected at the same time point in cohort 7 tumors ($n = 5$). This is an expected finding since the INGN 241 vector is nonreplicative by design, but also points to the need for repeat dosing to sustain the desired proapoptotic effect. In this regard, it is significant that objective clinical responses were restricted to patients who received multiple injections of INGN 241 [14].

These responders produced robust IL-6, IL-10, and TNF-α cytokine responses, but otherwise manifested a biologic profile similar to that of patients with stable

doi:10.1016/j.ymthe.2004.09.021

disease in the same cohort. A limitation of our current analysis lies in an inability to assess fully differences in *in situ* biologic response, since injected tumors for cohort 8 were not biopsied until 30 days postinjection. Since other expected anti-tumor biologic activity of MDA-7 was also evident in other patient cohorts, further improved pharmacokinetics may be necessary to realize fully the therapeutic potential of INGN 241. Robust induction of anti-adenoviral antibodies was noted within 8 days after a single injection of INGN 241 and increased by day 15 (Fig. 7C). We could not detect any correlation between either preexisting or induced anti-Ad antibodies and MDA-7 transgene expression, apoptosis induction, or anti-tumor responses. Thus high levels of anti-Ad antibodies do not appear to block either transduction by INGN 241 after intratumoral injection or anti-tumor activity upon repeat administration of INGN 241. No clinical sequelae were evident as a result of high titers of anti-Ad antibodies (up to 1/32,768).

Because of the diversity of tumor types sampled in this study, we cannot identify specific tumor types that do not respond to INGN 241. In Table 3, we summarize the biological analyses by tumor type and find that all tumors evaluated showed significant MDA-7 expression and apoptosis induction. Additional biologic markers of MDA-7 activity, regulation of β-catenin, iNOS, cytokine release, and angiogenesis, were observed in diverse tumor types, paralleling the preclinical studies. These data, from a limited set of human tumors, suggest that INGN 241 may have broad applicability.

The quantitative assays employed in this study demonstrate that up to 3% of vector distributes systemically within 30 min of intratumoral injection (Fig. 6). From these data, we can determine that the predicted half-life of INGN 241 vector DNA in human plasma is 11 min. Note that vector was not injected directly into the circulation, but appears to spill rapidly from the tumor into the circulation. The tumor does not appear to function as a depot or reservoir for vector release as circulating vector levels fall exponentially (Fig. 6A). Furthermore, because we have sampled the entire injected tumor, we can determine that up to 23% of injected vector is retained within the tumor at 24 h (average 11.75%; $n = 4$, Fig. 5B), and more than 99% of intratumoral vector DNA is lost by 4 days after injection. Comparing the total tumor vector DNA yields over time, we can predict that the half-life of intratumoral vector DNA is approximately 8 h. Clearly, vector DNA within tumors is much more stable than in the circulation. In contrast, intratumoral MDA-7 transgenic protein levels are stable and increase from 1 to 4 days (Fig. 1C), indicating that MDA-7 protein is much more stable than vector DNA and likely persists for more than 4 days. Although high levels of INGN 241 were detectable in the circulation (mean 2.2×10^7 DNA copies/ml), no pathology was attributed to circulating vector.

Lessons from this and other clinical trials validate the need to sustain the therapeutic dose of anti-tumor transgenes through repeat injections [36]. Alternatively, improved efficacy may be attained by using INGN 241 as an adjuvant to chemo/radiotherapy [10,18,25,32,37,38] in light of the capacity of MDA-7 to modulate multiple tumor suppressor gene and proto-oncogene pathways. Sustained and systemic expression of *mda-7* may also be attained through delivery with an oncolytic adenovector that selectively replicates in human cancer cells [26] or via nonviral delivery of *mda-7* [39]. Recent data indicate that INGN 241 can kill tumor cells via intracellular as well as extracellular mechanisms [27,33,40]. It is likely that the wide distribution of vector and transgenic MDA-7 observed in this study will facilitate greater "bystander" activity and, ultimately, provide improved patient benefit.

MATERIALS AND METHODS

Clinical protocol. An open-label, Phase I, dose-escalation study was conducted to evaluate the safety and determine the maximum tolerated dose of the adenovirus *mda-7* construct INGN 241 (Ad-mda7), when administered intratumorally to advanced cancer patients. The pharmacokinetics of INGN 241 DNA and RNA, MDA-7 protein, and humoral immune response to INGN 241 were evaluated to understand better their effects on both safety and efficacy.

Eligible patients with defined entry criteria [14] were enrolled into one of eight treatment cohorts (Table 1) and the dominant, symptom-causing tumor was identified and treated as the indicator tumor. The first two cohorts (one patient each) received 2×10^{10} or 2×10^{11} vp (cohort 2). Excisional biopsies were obtained at 24 h posttreatment. Cohorts 3, 4, and 5 (three patients per cohort) received 2×10^{12} vp and had excisional

TABLE 3: INGN 241 induces biologic effects in various tumor types

Tumor type	Dose	Apoptosis at center[a]	Apoptosis at periphery	Biologic activity[b]
Breast carcinoma	2×10^{10} vp	++	+	T, b, K
Colorectal carcinoma	2×10^{11} vp	+++	+	T, b, I, K
Melanoma	2×10^{12} vp	++	–	T, b, I, C
Breast	2×10^{12} vp	+++	++	T, b, K
SCCHN	2×10^{12} vp	+++	++	T, b, C, K
Adrenal carcinoma	2×10^{12} vp	+++	+	T, b
Hepatoma	2×10^{12} vp	+	–	T, b, C

[a] TUNEL reactivity: –, <5%; +, 5–19%; ++, 20–49%; +++, >50%.

[b] Biologic activity defined as T, TUNEL reactivity; b, β-catenin redistribution/decrease; I, iNOS down-regulation; C, CD31 down-regulation; K, decreased Ki-67 staining.

biopsies at 24 (cohort 3), 48 (cohort 4), and 96 h (cohort 5), respectively. Each resected lesion was serially sectioned and analyzed to determine the radius of diffusion of injection solution, distribution and concentration of the viral agent, transgene protein expression, and resulting biologic outcome. One patient was enrolled into cohort 6 and receive 2×10^{12} vp in divided doses administered to different sections of the indicator tumor, and excisional biopsies were obtained at 48 h.

To assess longer term effects of MDA-7 expression, five patients with unresectable disease were entered into cohort 7 and received 2×10^{12} vp and underwent incisional or core biopsies at pretreatment and at 30 days posttreatment. Cohort 8 included five patients who received single injections of 2×10^{12} vp twice a week for 3 weeks (total of six injections per cycle). All patients were analyzed throughout the trial for development of toxicity that may be related to either the agent or the injection. The clinical protocol was approved by the U.S. Oncology Institutional Review Board (IRB). All human subjected-related protocols for laboratory analyses that were performed at Baylor University Medical Center were reviewed and approved by the IRB for Human Protection at Baylor University Medical Center.

INGN 241 (Ad-mda7). INGN 241 comprises a replication-defective Ad5 backbone with E1 and partial E3 deletions. An expression cassette comprising the CMV immediate early promoter, the wild-type *mda-7* transgene ORF, and the SV40 polyadenylation sequence were cloned into the E1 region of the construct. Vector was double plaque purified and correct sequence confirmed as described [2]. Clinical material was prepared under current Good Manufacturing Practices (cGMPs) and complied with guidelines for testing for freedom from adventitious agents [14]. INGN 241 was provided as a frozen vial suspension (3.0 ml, 1×10^{12} vp/ml) in a neutral buffer containing saline and 10% glycerol. The vials were thawed to ambient temperature and mixed with a tracking dye (Isosulfan blue) immediately prior to injection.

Immunohistochemical analysis. A previously described automated immunoperoxidase staining technique [28] was used to characterize MDA-7 protein expression. Briefly, serial sections of formalin-fixed, paraffin-embedded tissue block were deparaffinized in xylene and graded alcohols. Antigen retrieval was carried out in 0.01 M citrate buffer in the microwave (Target Retrieval Solution, pH 6.0; Dako, Carpintevia, CA, USA). MDA-7 expression was determined using the avidin–biotin-complexed immunoperoxidase reaction (DAB Detection Kit; Ventana Medical Systems, Tucson, AZ, USA) following initial incubation with affinity-purified rabbit anti-human MDA-7 antibody (Introgen Therapeutics), using the Ventana 320ES System (Ventana Medical Systems). The reaction was compared with a negative control antibody stained slide and graded in a blinded fashion. Ad-mda7-transduced cells were used as a positive control. The frequency of immunoreactive cells was determined as an averaged value of the proportion of positive cells in three 100× power microscopic fields of representative staining pattern. Tumor cell types were distinguished from normal cells and/or infiltrating lymphoid cells by histological criteria by a trained histopathologist.

Determinations of β-catenin, iNOS, and CD31 expression were carried out in the same manner, following treatment with the relevant primary antibody (mouse anti-human β-catenin antibody C19220, 2.5 μg/ml, BD Biosciences; mouse anti-human iNOS monoclonal antibody N32020, 5 μg/ml; BD Pharmingen).

Quantification of apoptosis by TUNEL. A TUNEL method (DeadEnd Colorimetric Apoptosis Detection System; Promega) was used to detect DNA fragmentation *in situ*. Briefly, tissue sections were deparaffinized in xylene/graded alcohol and fixed in 4% paraformaldehyde in PBS before and after proteinase K treatment (20 μg/ml, 15 min, 23°C). An *in situ* terminal deoxynucleotidyl transferase reaction was carried out with biotinylated nucleotides according to the manufacturer's protocols. Apoptotic cells were identified by light microscopy as cells with definitive brown staining in the nucleus that were rounded or shrunken.

Serum cytokine analysis. ELISAs (R&D Quantikine Kit; Minneapolis, MN, USA) were used to quantify patient serum cytokine levels at defined time points before and after treatment as described previously [29]. Briefly, patient peripheral blood was collected by venipuncture. Serum samples were extracted after clotting and stored at −80°C. Serial serum samples from the same patient were analyzed simultaneously, using cytokine-specific immunoassay reagents according to the manufacturer's protocols. The colorimetric reaction was quantified as a function of OD absorbance at 540 nm (SpectraMax 340; Molecular Devices, Sunnyvale, CA, USA). Cytokine concentration was calculated according to a reference standard curve and OD values of known, graded concentrations of the recombinant cytokine. The minimal detectable concentrations, defined by OD reading at greater than or equal to threefold higher than background, are as follows: IFN-γ, <3 pg/ml; TNF-α, <4 pg/ml; IL-1β, <1 pg/ml; IL-10, <2 pg/ml; IL-2, <7 pg/ml; IL-6, <0.7 pg./ml; GM-CSF, < 3 pg/ml. The percentage increase in cytokine level at any time point posttreatment was determined through comparison with the baseline level in serum harvested before INGN 241 injection. Based on inter- and intrasample variations, increases in cytokine level of ≥50% over baseline were considered significant.

Flow cytometric immunophenotype analysis. Peripheral blood immunophenotype analysis was carried out by a two-color immunofluorescence reaction and flow cytometric analysis as described previously [30]. Briefly, patient or normal healthy donor peripheral blood was collected by venipuncture. One hundred microliters of whole blood was treated with 20 μl of the following reactant mixtures to determine the frequency distribution of T, B, and NK cell subsets: CD45-FITC/CD14-PE, CD3-FITC/CD19-PE, CD4-FITC/CD8-PE, CD13-FITC, CD20-FITC, CD56-FITC (all from BD Biosciences). The reactants were fixed with 1% paraformaldehyde before flow cytometric analysis (Becton–Dickinson FACScan) with the CellQuest software (Becton–Dickinson).

Anti-adenovirus antibodies. Serum samples were evaluated for anti-adenovirus type 5 antibodies using an indirect immunofluorescence assay to detect humoral immune responses against vector as previously reported [19]. Posttreatment samples were compared to baseline pretreatment anti-Ad antibody titers (defined as 1). Median pretreatment anti-Ad titers were 1/256.

Detection of viral DNA and RNA. Tumor samples were evaluated for the presence of INGN 241 DNA, mRNA expression from INGN 241, and expression of a panel of cytokine genes using real-time PCR, TaqMan chemistry, and the ABI Prism 7700 Sequence Detection System. A real-time PCR method was developed to target the junction of the vector CMV promoter with the 5′ end of the *mda-7* cDNA. The amplified product was specific for vector *mda-7* DNA and did not detect endogenous *mda-7*. Each specimen's DNA was analyzed in duplicate reactions containing 100 ng total DNA. A third reaction was spiked with 100 copies of the target to check for inhibitors of the PCR. Quantitation of vector DNA copies per cell used a conversion of 1×10^5 cellular genomes per microgram of genomic DNA. INGN 241-derived RNA was measured using a two-step RT-PCR method. First, cDNA was generated from total tumor RNA in a reverse transcription reaction primed with random hexamers. The cDNA was then amplified using the INGN 241 qPCR assay. The number of copies of INGN 241 transcripts per microgram of total RNA was calculated using a standard curve of INGN 241 in vitro runoff transcripts. The expression of tumor mRNAs for human interleukin-6, interleukin-10, and interferon-γ was determined using Applied Biosystems assay reagents. Expression of each cytokine was analyzed relative to the expression of human GAPDH.

INGN 241 qPCR assay primers and probe sequences. Primer and probe sequences were as follows: forward primer, CCCGTAATAAGCTTGGTACCG; reverse primer, TAAATTGGCGAAAGCAGCTC; probe, FAM–TGGAATTCGGCTTACAAGACATGACTGTG–TAMRA.

ACKNOWLEDGMENTS

The authors thank Dr. Joseph Newman at the Baylor University Medical Center (Dallas, TX, USA) for his assistance in flow cytometric analysis, Dr. Stefan Riedel of the Department of Pathology, Baylor University Medical Center, for his expertise in the histopathologic evaluation of patient biopsies, and Drs. William Hyman, Donald A. Richards, and Svetislava Vukelja of the Tyler Cancer Center

doi:10.1016/j.ymthe.2004.09.021

(Tyler, TX, USA) for their participation in the trial. This work was supported by NCI grants CA88421 and CA097598 (SC); RO1-CA102716, by the Texas Higher Education Coordinating Board ATP/ARP grant 003657-0078-2001, by an institutional research grant from The University of Texas M.D. Anderson Cancer (RR) and R41-CA 89778 and R42-CA 89778 (EAG and SC); and RO1-CA090282 (EAG).

RECEIVED FOR PUBLICATION FEBRUARY 22, 2004; ACCEPTED SEPTEMBER 22, 2004.

REFERENCES

1. Jiang, H., Su, Z. Z., Lin, J. J., Goldstein, M. I., Young, C. S., and Fisher, P. B. (1996). The melanoma differentiation associated gene mda-7 suppresses cancer cell growth. *Proc. Natl. Acad. Sci. USA* **93:** 9160–9165.
2. Mhashilkar, A. M., *et al.* (2001). Melanoma differentiation associated gene-7 (mda-7): a novel anti-tumor gene for cancer gene therapy. *Mol. Med.* **7:** 271–282.
3. Lebedeva, I. V., Su, Z. Z., Chang, Y., Kitada, S., Reed, J. C., and Fisher, P. B. (2002). The cancer growth suppressing gene mda-7 induces apoptosis selectively in human melanoma cells. *Oncogene* **21:** 708–718.
4. Saeki, T., Mhashilkar, A., Chada, S., Branch, C., Roth, J. A., and Ramesh, R. (2000). Tumor-suppressive effects by adenovirus-mediated mda-7 gene transfer in non-small cell lung cancer cell in vitro. *Gene Ther.* **7:** 2051–2057.
5. Saeki, T., *et al.* (2002). Inhibition of human lung cancer growth following adenovirus-mediated mda-7 gene expression in vivo. *Oncogene* **21:** 4558–4566.
6. Sarkar, D., Su, Z. Z., Lebedeva, I. V., Sauane, M., Gopalkrishnan, R. V., and Lalerie, K. (2002). Mda-7 (IL-24) mediates selective apoptosis in human melanoma cells by inducing the coordinated overexpression of the GADD family of genes by means of p38 MAPK. *Proc. Natl. Acad. Sci. USA* **99:** 10054–10059.
7. Sauane, M., *et al.* (2003). Mda-7/IL-24 induces apoptosis of diverse cancer cell lines through JAK/STAT-independent pathways. *J. Cell. Physiol.* **196:** 334–345.
8. Cao, X. X., *et al.* (2002). Adenoviral transfer of mda-7 leads to BAX up-regulation and apoptosis in mesothelioma cells, and is abrogated by over-expression of BCL-XL. *Mol. Med.* **8:** 869–876.
9. Caudell, E. G., *et al.* (2002). The protein product of the tumor suppressor gene, melanoma differentiation-associated gene 7, exhibits immunostimulatory activity and is designated IL-24. *J. Immunol.* **168:** 6041–6046.
10. Su, Z. Z., *et al.* (2003). Melanoma differentiation associated gene-7, mda-7/IL-24, selectively induces growth suppression, apoptosis and radiosensitization in malignant gliomas in a p53-independent manner. *Oncogene* **22:** 1164–1180.
11. Mhashilkar, A. M., *et al.* (2003). MDA-7 negatively regulates the beta-catenin and PI3K signaling pathways in breast and lung tumor cells. *Mol. Ther.* **8:** 207–219.
12. Ramesh, R., Ito, I., Saito, Y., Mhashilkar, A., Branch, C. D., and Chada, S. (2004). Overexpression of the melanoma differentiation associated-7 (mda-7)/interleukin-24 (IL-24) gene impairs lung cancer cell migration by modulating matrix metalloproteinase-2 (MMP-2) and E-cadherin expression. *Mol. Ther.* **9:** 510–518.
13. Ramesh, R., *et al.* (2003). Melanoma differentiation-associated gene 7/interleukin (IL)-24 is a novel ligand that regulates angiogenesis via the IL-22 receptor. *Cancer Res.* **63:** 5105–5113.
14. Cunningham, C. C., *et al.* (2004). Clinical and local biological effects of an intratumoral injection of mda-7 (INGN 241) in patients with advanced carcinoma: a Phase I study. *Mol. Ther.* (in press).
15. Ekmekcioglu, S., *et al.* (2003). Negative association of melanoma differentiation-associated gene (mda-7) and inducible nitric oxide synthase (iNOS) in human melanoma: MDA-7 regulates iNOS expression in melanoma cells. *Mol. Cancer Ther.* **2:** 9–17.
16. Huang, E. Y., *et al.* (2001). Genomic structure, chromosomal localization and expression profile of a novel melanoma differentiation associated (mda-7) gene with cancer specific growth suppressing and apoptosis inducing properties. *Oncogene* **20:** 7051–7063.
17. Su, Z. Z., *et al.* (1998). The cancer growth suppressor gene mda-7 selectively induces apoptosis in human breast cancer cells and inhibits tumor growth in nude mice. *Proc. Natl. Acad. Sci. USA* **95:** 14400–14405.
18. Yacoub, A., *et al.* (2003). Mda-7 (IL-24) inhibits growth and enhances radiosensitivity of glioma cells in vitro via JNK signaling. *Cancer Biol. Ther.* **2:** 347–353.
19. Nemunaitis, J., *et al.* (2000). Adenovirus-mediated p53 gene transfer in sequence with cisplatin to tumors of patients with non-small cell lung cancer. *J. Clin. Oncol.* **18:** 609–622.
20. Kubo, H., *et al.* (2003). Phase I dose escalation clinical trial of adenovirus vector carrying osteocalcin promoter-driven herpes simplex virus thymidine kinase in localized and metastatic hormone-refractory prostate cancer. *Hum. Gene Ther.* **14:** 227–241.
21. Ekmekcioglu, S., *et al.* (2000). Inducible nitric oxide synthase (iNOS) and nitrotyrosine (nt) in human metastatic melanoma tumors correlate with poor survival. *Clin. Cancer Res.* **6:** 4768.
22. Kotenko, S. V. (2002). The family of IL-10-related cytokines and their receptors: related, but to what extent? *Cytokine Growth Factor Rev.* **13:** 223–240.
23. Nemunaitis, J., *et al.* (2003). Pilot trial of intravenous infusion of a replication-selective adenovirus (ONYX-015) in combination with chemotherapy or IL-2 treatment in refractory cancer patients. *Cancer Gene Ther.* **10:** 341–352.
24. St George, J. A. (2003). Gene therapy progress and prospects: adenoviral vectors. *Gene Ther.* **10:** 1135–1141.
25. Kawabe, S., Nishikawa, T., Munshi, A., Roth, J. A., Chada, S., and Meyn, R. E. (2002). Adenovirus-mediated mda-7 gene expression radiosensitizes non-small cell lung cancer cells via TP53-independent mechanisms. *Mol. Ther.* **6:** 637–644.
26. Nemunaitis, J. (2002). Live viruses in cancer treatment. *Oncology* **16:** 483–492.
27. Sieger, K. A., *et al.* (2004). The tumor suppressor activity of MDA-7/IL-24 is mediated by intracellular protein expression in NSCLC cells. *Mol. Ther.* **9:** 355–367.
28. Nemunaitis, J., *et al.* (1998). Prognostic value of K-ras mutations, ras oncoprotein and c-erbB-2 oncoprotein expression in adenocarcinoma of the lung. *Am. J. Clin. Oncol.* **21:** 155–160.
29. Nemunaitis, J., *et al.* (2001). Intravenous infusion of a replication-selective adenovirus (ONYX-015) in cancer patients: safety, feasibility, and biological activity. *Gene Ther.* **8:** 746–759.
30. Zhang, Y. A., Nemunaitis, J., Scanlon, K. J., and Tong, A. W. (2000). Anti-tumorigenic effect of a K-ras ribozyme against human lung cancer cell line heterotransplants in nude mice. *Gene Ther.* **7:** 2041–2050.
31. Tong, A. W., *et al.* (2000). Cellular immune profile of patients with advanced cancer before and after taxane treatment. *Am. J. Clin. Oncol.* **23:** 463–472.
32. McKenzie, T., Liu, Y., Fanale, M., Swisher, S. G., Chada, S., and Hunt, K. K. (2004). Combination therapy of Ad-mda7 and trastuzumab increases cell death in her-2/neu-overexpressing breast cancer cells. *Surgery* **136:** 437–442.
33. Chada, S., *et al.* (2004). MDA-7/IL-24 is a unique cytokine in the IL-10 family. *Int. Immunopharmacol.* **4:** 649–667.
34. Fisher, P. B., *et al.* (2003). mda-7/IL-24, a novel cancer selective apoptosis inducing cytokine gene. *Cancer Biol. Ther.* **2:** 24–38.
35. Pataer, A., *et al.* (2002). mda-7 induces apoptosis via upregulation of the double-stranded RNA dependent kinase PKR. *Cancer Res.* **62:** 2239–2243.
36. Chada, S., Mhashilkar, A., and Ramesh, R. (2003). Cytokine- and chemokine-based gene therapy for cancer. *Curr. Opin. Mol. Ther.* **5:** 463–474.
37. Nishikawa, T., Ramesh, R., Chada, S., and Meyn, R. E. (2004). Suppression of tumor growth and angiogenesis by adenovirus-mediated mda-7/IL-24 gene transfer in combination with ionizing radiation. *Mol. Ther.* **9:** 818–828.
38. Nishikawa, T., *et al.* (2004). Adenoviral-mediated mda-7 expression suppresses DNA repair capacity and radiosensitizes non-small cell lung cancer cells. *Oncogene* **23:** 7125–7131.
39. Ramesh, R., *et al.* (2004). Local and systemic inhibition of lung tumor growth after liposome-mediated mda-7/IL-24 gene delivery. *DNA Cell Biol.*, (in press).
40. Chada, S., *et al.* (2004). Bystander activity of Ad-mda7: human MDA-7 protein kills melanoma cells via an IL-20 receptor-dependent but STAT3-independent mechanism. *Mol. Ther.*, (in press).

doi:10.1016/j.ymthe.2004.09.019

Clinical and Local Biological Effects of an Intratumoral injection of *mda-7* (IL24; INGN 241) in Patients with Advanced Carcinoma: a Phase I Study

C. Casey Cunningham[1,*] Sunil Chada[2,†] James A. Merritt[2] Alex Tong[1] Neil Senzer[1] Yuan Zhang[1] Abner Mhashilkar[2] Karen Parker[2] Sasha Vukelja[3] Don Richards[3] Jill Hood[2] Keith Coffee[2] John Nemunaitis[1]

[1]*Mary Crowley Medical Research Center, Dallas, TX 75246, USA*
[2]*Introgen Therapeutics, Inc., Houston, TX 77030, USA, and U.S. Oncology, Houston, TX, USA*
[3]*Tyler Cancer Center, Tyler, TX, USA*

**To whom correspondence and reprint requests should be addressed at 5th Floor, Collins Building, 3535 Worth Street, Dallas, TX 75246, USA. Fax: +1 214 370 1886. E-mail: casey.cunningham@usoncology.com.*

†To whom correspondence and reprint requests should be addressed at Introgen Therapeutics, Inc., Houston, TX 77030, USA. E-mail: s. chada@introgen.com.

The melanoma differentiation-associated gene-7 (*mda-7;* approved gene symbol IL24) is a tumor suppressor gene whose expression induces selective apoptosis in tumor cells. To characterize the safety and biologic activity of *mda-7* gene transfer, we conducted a phase I trial using intratumoral injections of an adenovirus containing the *mda-7* construct (Ad-mda7; INGN 241; 2×10^{10} to 2×10^{12} vp) in 28 patients with resectable solid tumors. One hundred percent of injected lesions demonstrated INGN 241 vector transduction, transgenic mRNA, elevated MDA-7 protein, and apoptosis induction, with the highest levels near the injection site. Apoptosis of cells in injected tumors was consistently observed even in heavily pretreated patients. INGN 241 vector DNA and mRNA were detected more than 1 cm from the injection site, whereas MDA-7 protein and bioactivity were more widely distributed. Toxicity attributable to the injections was self-limiting and generally mild; however, one patient experienced a grade 3 SAE possibly related to the study drug. Evidence of clinical activity was found in 44% of lesions with the repeat injection schedule, including complete and partial responses in two melanoma patients. Thus intratumoral administration of INGN 241 is well tolerated, induces apoptosis in a large percentage of tumor cells, and demonstrates evidence of clinically significant activity.

Key Words: *mda-7*, IL-24, apoptosis, bystander, ER, stress, cytokine, secretion, adenovirus, cancer gene therapy, IL-10, IL-19, IL-20, IL-22, receptor

INTRODUCTION

The melanoma differentiation-associated gene-7 (*mda-7*; approved gene symbol IL24) is a tumor suppressor gene identified by subtraction hybridization from human melanoma cells induced to terminally differentiate by IFN-β and mezerein [1]. The *mda-7* cDNA encodes a novel 24-kDa protein with low amino acid homology to interleukin 10 (IL-10) and greater homology to the IL-10 family members: IL-19, IL-20, IL-22, and IL-26 [2,3]. Based upon its localization within the IL-10 family cluster at 1q32.2 and cytokine-like properties, *mda-7* was designated by HUGO as interleukin 24 [4]. The MDA-7 protein contains a consensus signal sequence and proteolytic cleavage site and *mda-7*-transfected cells secrete a soluble form of the protein [3,5].

Expression of MDA-7 by adenoviral gene transfer (Ad-mda7; INGN 241) induces apoptotic cell death in cells from a variety of solid tumor types, including melanoma, lung, breast, colorectal, and prostate [3,5–11]. However, the mechanism by which apoptosis occurs varies, depending upon the cell type studied. Further investigations of MDA-7-induced apoptosis are ongoing, but the process is clearly independent of p53, Rb, Ras, Bax, and caspase 3 [5,8]. Significantly, levels of expression of MDA-7 similar to those that induce apoptosis in tumor cells have little or no effect in normal human mammary epithelial cells,

1525-0016/$30.00

doi:10.1016/j.ymthe.2004.09.019

human skin fibroblasts, human endothelial cells, or rat embryo fibroblasts [3,11], implying selective activity limited to malignant cells. *mda-7* gene transfer thus offers promise as a new and potentially widely applicable antitumor therapeutic.

Preclinical animal models support this promise. Inhibition of tumorigenicity was seen in a model using *ex vivo* treatment of the breast cancer line MCF-7 with *mda-7* gene transfer [9]. Intratumoral injections of INGN 241 into subcutaneous xenografts of H1299 or A549 lung cancer cells in nude mice demonstrated significant tumor growth inhibition and apoptotic tumor cell death compared to control injections [10,12]. The injected tumors were removed after 48 h and exhibited colocalization of MDA-7 protein and apoptotic marker expression. Intratumoral injection of INGN 241 into Her-2/neu overexpressing breast cancer xenografts resulted in significant inhibition of tumor growth [13]. No toxic effects of INGN 241 administration in these pharmacology studies were identified. GLP toxicology studies of INGN 241 in mice found effects only at the highest dose (5×10^{12} viral particles (vp)/kg; equivalent to a human dose of 3×10^{14} vp), which consisted of decreases in body weight, mild liver toxicity, and transient decreases in platelet counts (unpublished data). Therefore, to begin to characterize the safety and biologic activity of *mda-7* gene transfer in a clinical setting, we conducted a phase I trial using intratumoral injections of INGN 241 into resectable solid tumor lesions. In this report, we detail our findings from that study.

RESULTS

Patient Characteristics and Safety Analyses After INGN 241 Treatment

After study entry, all patients underwent a baseline biopsy procedure to provide control uninjected tumor. We treated patients in a prespecified dose-escalation schema and they received 2×10^{10} to 2×10^{12} vp delivered into the central region of the target tumor; injected tumors were resected to evaluate efficiency of gene transfer and biologic endpoints (Fig. 1). Twenty-eight patients were enrolled in the trial; 22 patients completed at least one cycle of treatment (Table 1). Patients included 13 females and 9 males and ranged in age from 38 to 92, with a median age of 66. Date of initial cancer diagnosis ranged from 1982 to 2002; all patients had been heavily pretreated as shown in Table 1. The majority had received surgery in addition to chemotherapy and/or radiotherapy. The inclusion criteria for this study allowed enrollment of patients with a variety of solid tumors. A total of 15 different tumor types were enrolled in the study: melanoma, breast, SCCHN, colorectal, lymphoma, hepatoma, NSCLC, adenocarcinoma, sarcoma, and carcinomas of the adrenal, bladder, parotid, lip, kidney, and penis. Malignant melanoma (21.4%), SCCHN (18%), breast carcinoma (14%), and colorectal carcinoma (7%) were the most frequent tumor types. Adverse events were generally mild (Table 1); however, there was one grade 3 serious adverse event (SAE) involving fatigue in a cohort 8 patient that was possibly related to the study drug. We removed this patient from the study. We observed no other SAEs considered possibly related to INGN 241. Of the adverse events specifically related to injection of the study drug, the most common were injection site pain and fever, ≤ 2, occurring within 24 h of tumor injection. We saw these effects more consistently at higher doses of INGN 241 and they generally resolved by 48 h postinjection. In two patients in cohort 8 (twice-weekly injections), we noted marked skin erythema surrounding the injected lesion within 24 h of injection. This then resolved over the following 96 h. A maximum tolerated dose was not attained in this study. Overall, the accumulated data from 22 patients completing treatment indicate that INGN 241 is well

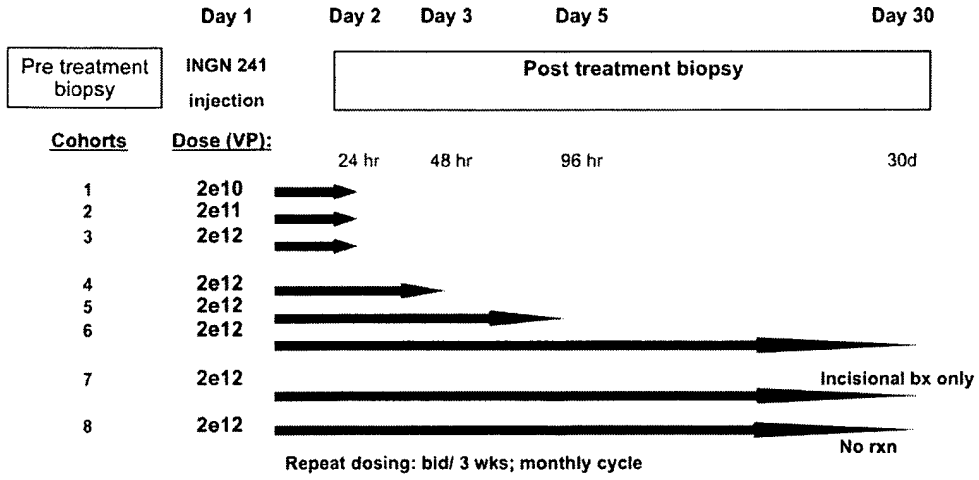

FIG. 1. Study schema for clinical protocol. The dose levels of INGN 241 and biopsy schedules are indicated. bx, biopsy; rxn, resection.

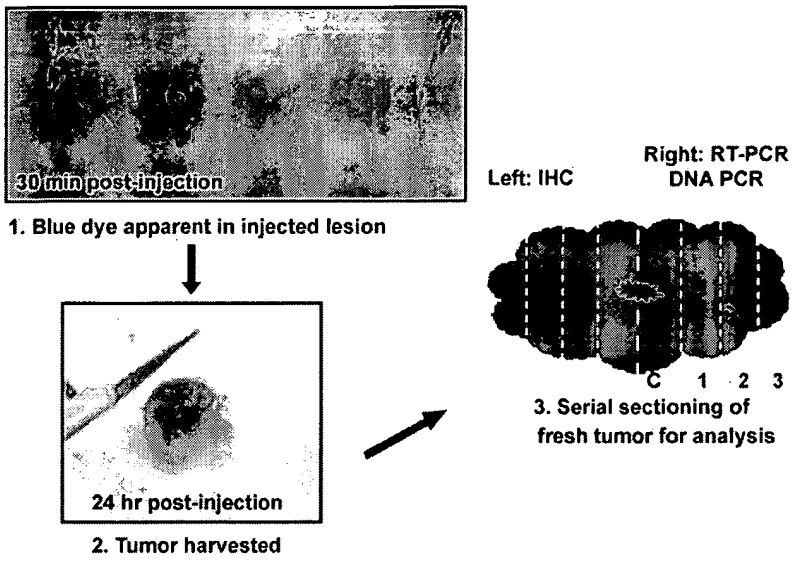

FIG. 2. Excisional biopsy procedure. (1) INGN 241 vector admixed with Isosulfan blue allows identification of the site of injection. (2) Lesion resected 24 h after injection. (3) Postresection processing. The bisected lesion is serially sectioned and the left portion is fixed and evaluated by immunohistochemistry. The right half is sectioned and immediately flash-frozen for quantitative PCR analyses.

tolerated when administered in single or multidosing regimens.

Vector Distribution and Kinetic Profiles After Injection

We analyzed gene transfer and biologic effects elicited by intratumoral injection of INGN 241 in cohorts 1–5 (patients 1–12), in which we resected tumors after 1–4 days. Treated tumors ranged in size from 1.8 × 1.2 to 11.0 × 8.1 cm (average area was 22.7 cm^2). We performed quantitative analyses of vector-specific DNA and RNA at the point of injection (center of lesion) and in serial sections to the periphery of each lesion. To facilitate identification of the injection site, we admixed Isosulfan blue dye with vector just prior to administration. Upon resection of tumors (1–4 days later), injec-

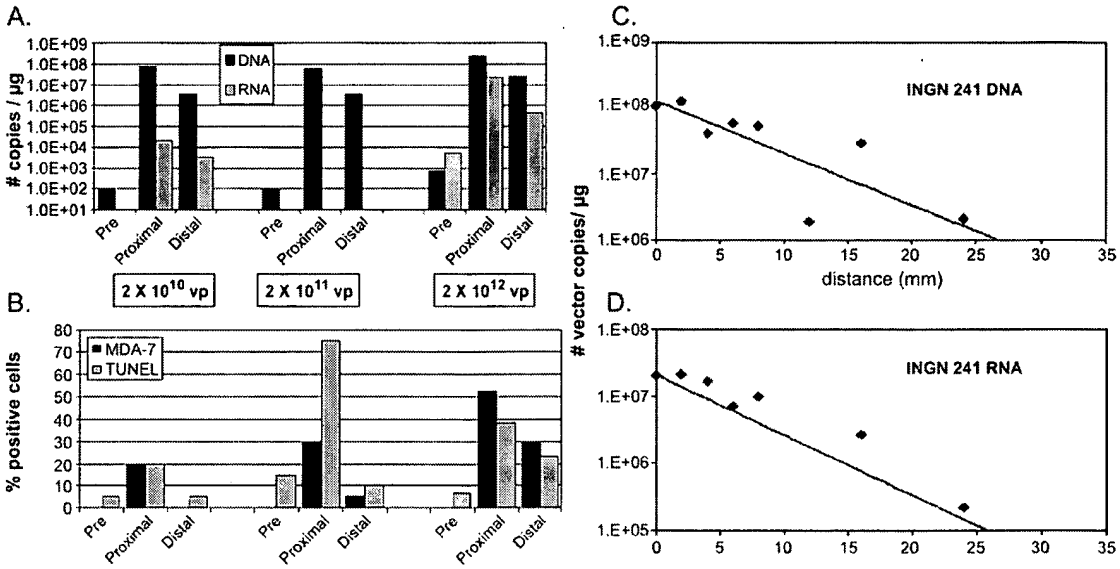

FIG. 3. Pharmacodynamics of INGN 241 vector and expression. (A) Dose response of INGN 241 vector DNA and RNA. Tumor sections were obtained from preinjected (Pre), proximal, and distal sections from cohort 1–3 patients and vector-specific signals evaluated by quantitative DNA- and RT-PCR. RNA was not available from cohort 2 tumor. (B) Dose response of INGN 241 transgenic MDA-7 expression and TUNEL reactivity. Tumor sections were obtained from preinjected (Pre), proximal, and distal sections from cohort 1–3 patients and vector-specific signals evaluated. (C) Spread of INGN 241 DNA and (D) RNA from injection site. Genomic DNA and RNA were isolated from tumor sections and analyzed using vector-specific primers for INGN 241. Signals were quantitated using real-time PCR. Data are plotted to indicate signals compared to distance from injection site. Correlation coefficient for DNA decay = 0.9 ($P < 0.02$) and for RNA decay = 0.82 ($P < 0.05$). ($n > 40$ samples were used in the analysis.)

doi:10.1016/j.ymthe.2004.09.019

tion sites could be identified by the intense blue staining (Fig. 2). Pretreatment (uninjected) lesions exhibited low vector PCR signals: median pretreatment samples contained 100 vector DNA copies/μg tumor genomic DNA, whereas these lesions had 213 RNA copies/μg tumor RNA. All injected lesions showed high levels of vector-specific DNA signals in tumors (Fig. 3). We compared vector DNA, vector RNA, transgenic MDA-7, and TUNEL signals across the dose range of 2×10^{10}–2×10^{12} vp (Figs. 3A and 3B). Although the sample size was small, there was indication of a dose-dependent increase in the number of INGN 241 vector DNA copies/μg DNA in the tumor (7×10^7 copies/μg in the proximal (central) sections of cohort 1 compared to an average of 2.2×10^8 copies/μg in cohort 3). We observed a similar indication of dose response for vector RNA, with 2.0×10^4 vector RNA copies found in the central section of tumors injected with low dose INGN 241, whereas 2.3×10^7 copies/μg were observed in high-dose tumors (Fig. 3A). Note that the distal regions of tumors uniformly showed lower vector signals than the proximal sections. We evaluated parallel sections for transgenic MDA-7 protein and apoptosis induction via TUNEL assay. All patients demonstrated undetectable MDA-7 staining in the preinjected baseline samples, whereas we found MDA-7 immunostaining in 20% of tumor cells from low dose, 30% of cells at intermediate dose, and 53% of cells from tumors injected with high dose of INGN 241. We did not observe MDA-7 staining in distal regions of tumors injected with low dose vector, whereas we found 5 and 30% positive cells in mid- and high-dose tumors, respectively. Apoptosis induction also trended higher with increased dose, except for the cohort 2 patient (colorectal carcinoma) who exhibited unusually high TUNEL reactivity of 75% after injection of INGN 241 (Fig. 3B).

We evaluated the dynamics of vector spread and subsequent gene expression. We found the highest number of DNA vector copies at the area of injection (e.g., the center of injected lesions averaged greater than 1×10^8 vector DNA copies/μg) and signal decreased significantly ($P < 0.02$) with distance from the injection site; 1 cm from the injection site, vector DNA levels had fallen by almost 90% (Fig. 3C). We could detect low levels of vector DNA up to 3 cm from the injection site; however, only 3 tumors showed DNA signals greater than 1×10^6 copies/μg at 1 cm from the injection site. We also quantitated vector RNA levels and they showed a pattern of distribution similar to that of the vector DNA (Fig. 3D). Vector RNA also was distributed distally from the injection site and, similar to vector DNA, vector RNA signals were significantly reduced ($P < 0.05$) with distance from the injection site. Both vector DNA and RNA signals showed exponential decay with distance from the injection site (correlation coefficient = 0.82–0.9).

We evaluated the kinetics of vector DNA and transgenic mRNA for patients who received a single dose of INGN 241. Vector DNA reached maximum levels at the point of injection 24–48 h after injection. If one assumes these signals are cell-associated, then median signals approximated 1000 vector DNA copies per cell, a value 6 logs above preinjection controls (Fig. 4A). Vector DNA signals decreased by almost 3 logs by day 4 and by greater than 4 logs by day 30, although DNA was still detectable above background levels at 30 days after injection (Fig. 4A). Vector-specific mRNA exhibited a distribution and kinetic profile similar to that of vector DNA (Fig. 4B). Median vector-specific RNA signals were more than 4 logs greater in the center of injected lesions compared to uninjected control samples (Figs. 3A and 4B). Vector-specific RNA signals decreased by more than 2 logs by day 4 (Fig. 4B). Samples were not available for day 30 analysis.

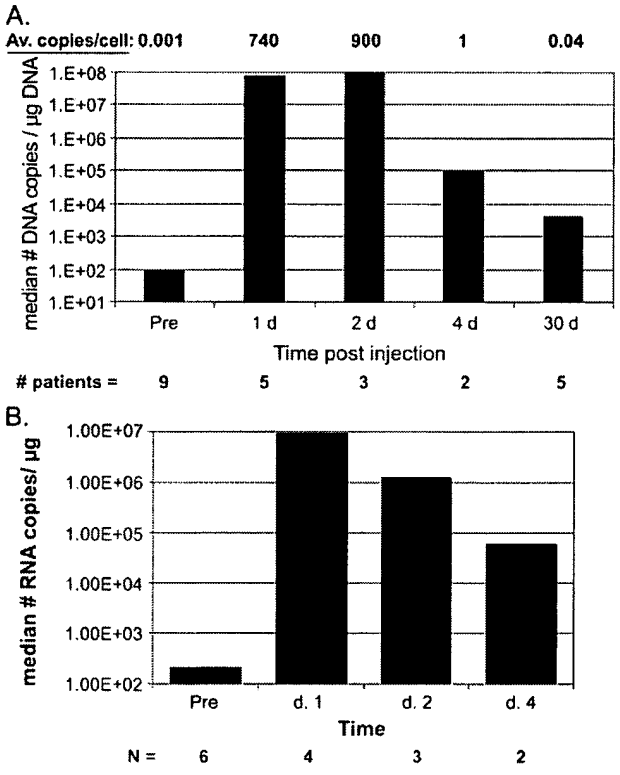

FIG. 4. Intratumoral pharmacokinetics of vector DNA and mRNA. (A) Decay of INGN 241 vector at injection site. The median number of DNA copies at each time point postinjection is shown; number of patients per sample is indicated below. The number of DNA copies/μg genomic DNA was converted to illustrate the average number of vector DNA copies per cell—shown above graph. (B) Decay of INGN 241 vector RNA at injection site. The median number of RNA copies/μg at each time point is shown; number of patients per sample is indicated below.

Transgenic Gene Expression After INGN 241 Injection

We serially sectioned excised tumors and evaluated them for transgenic MDA-7 protein expression and apoptosis. Pretreatment samples were uniformly negative for MDA-7 protein expression and most were negative for TUNEL reactivity (average TUNEL signal was <6% in cohorts 1–5). After INGN 241 injection, all tumors demonstrated substantial MDA-7 immunostaining that ranged from 20 to 90% positive tumor cells in the center of the lesion (Fig. 5A). We detected transgenic MDA-7 beyond the injection site: five of eight (62%) tumors had detectable MDA-7 at 1 cm from the single injection site, and MDA-7 expression was detected more than 3 cm from the injection site. We detected up to 25% MDA-7-stained cells 16 mm from the point of injection. Reproducibly, within each tumor MDA-7 immunostaining was reduced with distance from the injection site. With the exception of patient 2, ≥90% of MDA-7-staining cells in all biopsies exhibited malignant histological features. The remaining MDA-7-positive cells comprised infiltrating lymphocytes and/or histocytic/reticuloendothelial cells.

Apoptosis staining varied, with up to 80% of tumor cells at the center of the lesion demonstrating TUNEL reactivity. Apoptosis declined with distance from the injection site; five of seven (71%) tumors exhibited TUNEL reactivity beyond 1 cm from the injection site (Fig. 5B). Both MDA-7 and TUNEL staining demonstrated significant ($P < 0.02$) linear decay with distance from the injection site. Regions of tumor exhibiting TUNEL staining strongly corresponded to those regions having MDA-7 protein expression; those samples with distal MDA-7 staining also showed distal TUNEL reactivity. Both protein expression and apoptosis reactivity reached maximum levels by 4 days postinjection but had returned to baseline, preinjection levels by day 30 (31, data not shown).

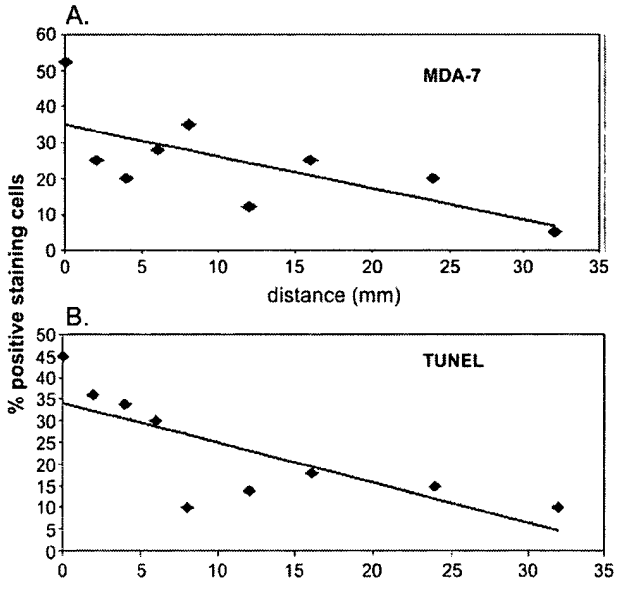

FIG. 5. Spread of MDA-7 protein and biological effect. MDA-7 protein expression correlates with apoptosis. Serial sections from each tumor were evaluated for (A) MDA-7 expression and (B) TUNEL reactivity using immunohistochemistry. Data are plotted to indicate signals compared to distance from injection site. Both MDA-7 and TUNEL staining show strong correlation with distance; correlation coefficient for MDA-7 = 0.69 and for TUNEL = 0.77 ($P < 0.02$). ($n > 30$ samples were used in the analysis.)

A representative example is shown in Fig. 6, which illustrates the high level of MDA-7 immunostaining after INGN 241 injection and the decay in protein, DNA, and RNA signals with distance from injection site. This patient with a 5 × 5 cm SCCHN lesion was injected with 2×10^{12} vp INGN 241 and resected at 24 h. We observed no MDA-7 signal in the pretreatment lesion, whereas the injection site (center section) exhibited up to 75% of tumor cells staining for MDA-7. Staining intensity decreased with distance, but the distal lesion (18 mm from injection site) still showed regions of strong MDA-7 staining (Fig. 6). Parallel sections were evaluated for apoptosis. The central section showed 50% TUNEL reactivity, whereas the distal section showed 30% staining. The levels of vector-specific DNA and RNA showed strong signals at the injection site, which decreased markedly (more than 1000-fold) at the periphery (Fig. 6). Overall, vector-specific DNA and RNA, MDA-7 protein levels, and TUNEL reactivity demonstrated similar dose response and kinetic and radial concentration gradients, although MDA-7 and TUNEL signals persisted longer and showed enhanced distribution.

Clinical Responses to INGN 241 Injection

In the first six patient cohorts, we excised the injected lesions 24 to 96 h after injection; therefore no conclusions about clinical activity can be drawn. Although we saw minor changes in morphology in the injected lesions of several cohort 7 patients, none qualified as an objective PR using RECIST guidelines. Tumor measurement data were available for only three cohort 7 patients at the end of study: the tumors exhibited SD (stable disease), with 0, 0, and 23% reduction in tumor size (melanoma, colorectal carcinoma, and SCCHN, respectively). Off-study tumor measurements were taken 5–7 weeks from screening. Time from first injection to death for these patients was 347, 51, and 401 days, respectively.

Cohort 8 patients received injections twice weekly for 3 weeks (in a 28-day cycle); five patients completed at least one cycle of treatment. All patients in this cohort had failed multiple prior therapies (Table 2). Two of five patients demonstrated a clinically significant response to INGN 241 injections consisting of at least partial regression of the injected lesion. The most dramatic of these responses was in a 64-year-old female with widely metastatic melanoma (at study entry, she

doi:10.1016/j.ymthe.2004.09.019

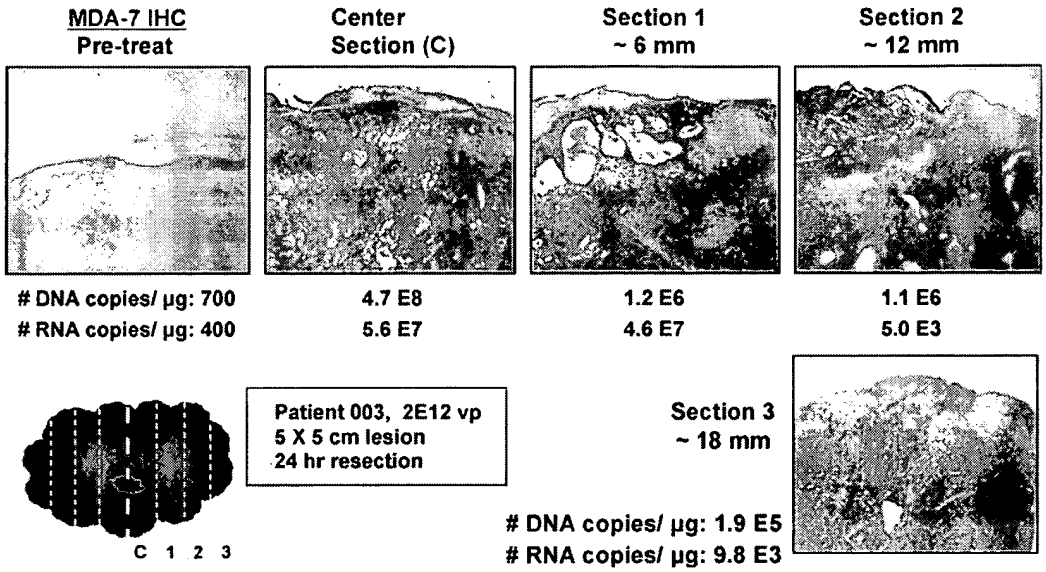

FIG. 6. MDA-7 transgene expression correlates with distribution of vector throughout the tumor. One-half of the tumor was analyzed for MDA-7 protein expression and the other half for vector-specific DNA and RNA levels. The number of DNA copies/µg genomic DNA and number of RNA copies/µg total RNA are shown for each tumor section. TUNEL reactivity was 50% in the central section and 30% at the periphery (Section 3).

had >10 distinct lesions). Her initial site of treatment was a supraclavicular node measuring 2 × 2 cm at baseline. No appreciable change was noted for the first five injections but by the sixth (and final) injection, a clear decrease in the size of the lesion was apparent and was associated with erythema over the anterior chest (Fig. 7). The erythema resolved and regression continued over the next 2 weeks until there was no clinical evidence of disease at that site (Fig. 7). Subsequently, we began a second course of injections on a lesion on the dorsum of the right hand. The baseline measurement was 1.8 × 2.3 cm and regression was evident by the fifth injection (84% reduction in lesion area). After completing six injections, we excised the residual lesion and on microscopic examination found it to have a marked inflammatory lymphoplasmacytic infiltrate throughout the residual nodule and surrounding tissue with extensive coagulative necrosis in the tumor. We then treated a third lesion on the anterior right thigh with two cycles of injections. We saw regression of this lesion also after the first course of injections (baseline measurements 3.5 × 3.25 cm decreasing to 2.4 × 3.1 cm after the injection course; 35% reduction in lesion area) but a second set of injections produced no further response. Interestingly, several distant uninjected melanoma lesions also became erythematous during the course of injection of the target lesion, although clinical regression was not seen at these distant sites. This patient is still alive >600 days after initiating INGN 241 treatment. An additional melanoma patient exhibited a partial response (33% decrease by RECIST).

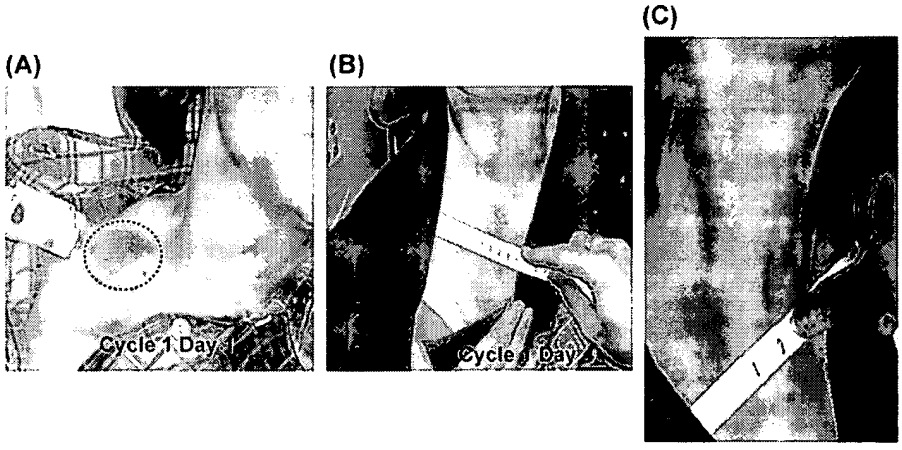

FIG. 7. Objective clinical response to INGN 241 in a patient with metastatic melanoma. Cohort 8 patient with metastatic melanoma. Injected lesion was on right clavicle (dashed circle in (A)). (B) By day 4, region is inflamed. (C) At the end of cycle 1 (day 30), lesion has completely regressed. This patient is still alive >600 days after initiating treatment.

TABLE 1: Patient characteristics and dosing

Cohort	No. of patients[a]	Age (range)	Previous treatments[b]	Dose (vp)	Adverse events[c]
1	1 (1)	49	S, C, Ca, N, H, G	2×10^{10}	2
2	1 (1)	44	S, F, I	2×10^{11}	1
3	3 (3)	74 (66–76)	S, RT, T, P, C, V, D, Fl, Cl	2×10^{12}	0/1/1
4	3 (3)	45 (38–60)	S, A, C, T, Ta, N, P, RT, E	2×10^{12}	0/1/0
5	4 (3)	75 (65–75)	S, Ta, RT, I, D	2×10^{12}	0/2/2
6	1 (1)	57	S, A, T, Ta	2×10^{12}/divided doses	0
7	7 (5)	86 (76–92)	S, M, V, A, P, T, G, RT, F, I	2×10^{12}	2/0/0/2/2
8	8 (5)	64 (62–91)	S, RT, IF, IT, P, T, F	2×10^{12} repeated 2×/week for 3 weeks	2/2/2/1/1/[d]

[a] Number of patients enrolled per cohort is indicated. The number of patients completing at least one cycle of treatment is shown in parentheses.
[b] Prior treatments: S, surgery; A, adriamycin; C, cyclophosphamide; Ca, capecitabine; Cl, chlorambucil; D, dacarbazine; E, etoposide; F, 5-fluorouracil; Fl, fludarabine; G, gemcitabine; H, herceptin; I, irinotecan; IF, IFN-α; IT, immunotherapy; M, methotrexate; N, navelbine; P, platinum; RT, radiotherapy; T, taxane; Ta, tamoxifen; V, vincistine.
[c] Adverse events possibly or probably related to INGN 241 administration are indicated.
[d] One cohort 8 patient experienced a grade 3 SAE and withdrew from the study.

We saw a less dramatic response in another patient with squamous cell carcinoma of the penis with multiple skin nodules in the groin and right hip area. Injection of INGN 241 into one of the upper right hip lesions (2.5 × 3.0 cm at baseline) produced significant central necrosis with surrounding erythema by the fifth injection. However, the lesion continued to expand peripherally so that by completion of the first set of six injections, there was an indurated rim of erythematous tissue surrounding the central area and the total measurement of the lesion was now 3.0 × 4.0 cm. A large central portion of the lesion (approximately two-thirds of the total area) remained blackened and necrotic at the end of cycle 1. Other, new lesions were rapidly appearing in the region, so we removed the patient from the study as PD and he went on to other therapy. Three additional patients (with adenocarcinoma, NSCLC, and lip carcinoma) exhibited stable disease after INGN 241 injection and one patient with SCCHN exhibited disease progression (20% increase by RECIST). Of the nine lesions treated in cohort 8 patients, four demonstrated objective response (CR or PR by RECIST criteria). Five patients are still alive 600–1160 days after INGN 241 injection.

Discussion

mda-7 is a tumor suppressor gene encoding a proinflammatory cytokine. *mda-7* gene transfer demonstrates potent growth arrest and cell death in a variety of preclinical tumor models [3,11]. Perhaps most significantly, expression of MDA-7 protein at levels giving rise to these anti-tumor effects does not produce similar cytotoxicity in a variety of normal cell lines. In this report, we detail the initial clinical experience with MDA-7 in patients with refractory cancer. Direct injection of an adenovirus containing the *mda-7* cDNA (INGN 241) into a variety of solid tumors was generally well tolerated, with injection site pain and erythema being noted locally in some patients. One patient experienced a grade 3 SAE of fatigue and was discontinued from study.

Analysis of serial sections of injected lesions demonstrated that MDA-7 DNA and RNA were detectable in 100% of the injected lesions, with the highest concentrations found at the site of injection, as expected (Fig. 3). However, MDA-7 protein was detectable in the periphery of injected lesions (greater than 3 cm from injection site), beyond the area of DNA spread, suggesting that the MDA-7 protein can diffuse from transduced cells (compare Figs. 3C, 3D, 5, and 6). Immunohistochemical staining of tumor sections showed regions of intense punctate MDA-7 staining surrounded by regions of more diffuse staining, which may be reflective of active secretion of MDA-7 from transduced cells (Fig. 6). These data are consistent with our preclinical studies in which we have demonstrated active secretion of glycosylated MDA-7 after INGN 241 transduction [5,17]. Glycosylated human MDA-7 mediates induction of immune, antiangiogenic, and cytotoxic bystander effects [3–5,18,30].

Apoptosis, as measured by TUNEL assay, was significant in the injected lesions and correlated geographically with MDA-7 protein expression (Figs. 5 and 6). Both MDA-7 transgenic protein expression and apoptosis decayed with similar intratumoral dynamics (compare Figs. 5 and 6). In lesions injected and then not biopsied until day 30, protein expression and apoptosis had returned to baseline levels (data not shown). Such a decrease is to be expected since the INGN 241 virus is nonreplicating, but also illustrates the need for repeat dosing to maintain levels of protein expression. In this regard, it is significant that the objective clinical responses were seen in the cohort of patients receiving repeat injections. If protein expression, and by extension apoptosis, is kinetically limited then repeat dosing will provide greater therapeutic benefit.

A unique feature of this study was the inclusion of Isosulfan blue as marker dye to localize injection site. The ability to identify precisely the injection site

doi:10.1016/j.ymthe.2004.09.019

facilitated comprehensive pharmacodynamic and kinetic analyses of vector distribution within human tumors. One hundred percent of injected tumors evaluated in our study demonstrated transgenic MDA-7 expression and elevated apoptosis induction compared to untreated control tumors. In contrast, adenoviral-mediated gene transfer of p53 by injection into non-small-cell lung tumors resulted in vector detection by DNA PCR in 86% of patients' tumors and increased apoptosis in 46% of biopsy specimens [19]. Indeed, as most previous gene transfer studies have not been structured to assess the geographic extent of vector distribution and biologic effect, it is difficult to compare INGN 241's effects directly with other studies. A recent report has indicated that administration of Ad-p53 to glioma is hampered by the limited spread (<5 mm) of transduced cells [20]. Both INGN 241 DNA and transgenic MDA-7 protein distribute to a greater extent (see Figs. 3, 5, and 6) and demonstrate strong correlations with distance from injection site ($P < 0.02$). Nucleic acid signals decay by 50% at 4–6 mm from the injection site whereas MDA-7 protein and apoptosis signals decay by 50% at 18–20 mm. Therefore, either INGN 241 is more potent than other therapeutic constructs at inducing apoptosis in human tumors or the study design allowed us to capture signals that were lost in other studies. The levels of apoptosis induction observed in this study are substantially higher (average = 45%) than reported with other anti-cancer drugs. Apoptosis induction correlates with loss of Ki-67 staining [31]. It is noteworthy that seven different tumor types were treated in cohorts 1–6 and all showed high levels of MDA-7 expression and subsequent apoptosis induction. As discussed above, all these patients had been heavily pretreated and failed multiple treatment regimens (Table 1). It would be predicted that this group of chemo- and radio-resistant tumors would have acquired resistance to apoptosis. The fact that MDA-7 induces apoptosis in such a spectrum of advanced tumor types mirrors our preclinical studies and suggests that INGN 241 may have broad utility.

MDA-7 (IL-24) also acts as an interleukin, stimulating IL-6, TNF-α, GM-CSF, and IFN-γ production [4]. An interesting avenue for further investigation is then the potential systemic immunomodulatory effects of intratumoral MDA-7 [3,29,32]. The significant apoptosis in concert with downregulation of TGF-β [10] suggests the potential for enhanced dendritic cell priming and maturation at the local injection site. We have previously demonstrated MDA-7 immunostaining in dendritic cells in human tumors and tonsil [3,21], and recent data indicate an adjuvant effect of *mda-7* gene transfer in syngeneic murine tumor models [3]. Therefore, it is intriguing that one patient developed erythema of distant lesions following injection of one primary site. If this represented an immune response, however, it was not robust enough to lead to clinical response of the distal lesions.

Preclinical studies evaluating activity of Ad-mda7 in various tumor models have revealed a complex interplay between direct tumor cell killing and other complementary (bystander) anti-tumor mechanisms. For example, Ad-mda7 is able to kill tumor cells by activating a variety of proapoptotic signaling pathways (p53, PKR, PTEN, TRAIL, JNK) and concomitantly inhibiting survival/oncogenic pathways (PI3K, bcl-2, β-catenin) [13,17,22–28]. MDA-7 can elicit death in tumor cells via either intracellular or extracellular pathways [17,30]. Ad-mda7 induces a stress response signal from the endoplasmic reticulum via caspases 7 and 12, leading to mitochondrial disruption and intrinsic apoptosis [17]. This pathway appears to predominate in cells that lack receptors for MDA-7. In cells expressing cognate MDA-7 receptors (IL-20R1/IL-20R2 and IL-22R1/IL-20R2), ligand engagement activates alternate signaling pathways that result in tumor cell death ([30], unpublished data). Thus human MDA-7 protein can kill tumor cells in either a receptor-dependent or a receptor-independent fashion. Recombinant MDA-7 produced from nonmammalian sources does not share

TABLE 2: Responses in cohort 8 patients

Patient	Gender/age	Diagnosis	Date diagnosed	Previous treatments	No. of injections	Response	Time to death[a]
81	M/71	Adeno-carcinoma	1998	Carboplatin/taxane/ gemzar	2[b]	SD	n.d.
83	F/64	Melanoma	1994	Surgery/RT/Immuno-tx/IFN-α	24[c]	CR, PR, SD	>600
84	F/62	Melanoma	2000	Surgery/RT/Immuno-tx/IFN-α	12	PR	309
85	M/64	Penile carcinoma	2002	Surgery, RT/CDDP/ taxane	6	PD	75
86	F/66	NSCLC	2001	RT/carboplatin/taxane	3[b]	SD	180
87	M/62	SCCHN	1992	Surgery/RT/CDDP/ taxane/ 5-FU/carboplatin	6	PD	185
88	M/91	Lip carcinoma	1982	Surgery/RT	6	SD	181

SD, stable disease; CR, complete response; PR, partial response; PD, progressive disease.
[a] Time in days from first injection of INGN 241 until death.
[b] Patients 81 and 86 did not complete one full course of treatment (6 injections).
[c] Patient received 12 injections on compassionate use protocol.

these properties [17,30]. The active secretion and receptor utilization of MDA-7 may help to explain both the wide distribution of ectopic MDA-7 in human tumors and the widespread radius of effect. We hypothesize that intratumoral injection of INGN 241 results in high local concentration of INGN 241 within tumors and diffusion of bioactive MDA-7 protein throughout the tumor. Furthermore, vector DNA and RNA signals decrease faster than MDA-7 protein and apoptosis (Figs. 3C, 3D, and 6), supporting a bystander activity for MDA-7 [30].

In addition to apoptosis induction of tumor cells and immunostimulation, additional bystander activities have been reported for MDA-7. Ad-mda7 was reported to inhibit endothelial differentiation *in vitro,* implying antiangiogenic activity [10]. Further studies demonstrated antiangiogenic activity of Ad-mda7 *in vivo* [12], in that MDA-7 expression significantly repressed angiogenic mediators, including VEGF, basic FGF, and IL-8. Studies using purified MDA-7 demonstrated that it functions via the IL-22R1 on endothelial cells [18] and MDA-7 was 50-fold more active than endostatin or angiostatin. When Ad-mda7 was combined with XRT, synergistic inhibition of tumor growth was observed, with significant reduction in microvessel density and pronounced apoptotic response in tumors [12]. Two recent preclinical studies have provided support for intriguing observations about the role of MDA-7 in melanoma disease progression and metastasis. Initial studies found that MDA-7 protein was expressed in normal human melanocytes and benign nevi, but expression was lost in metastatic melanoma [6]. Subsequent studies evaluated larger patient groups and concluded that MDA-7 protein expression is progressively lost as melanoma tumors invade and become more metastatic and aggressive [21]. These authors speculated that MDA-7 must play a role in maintenance of normal physiology of melanocytes and that inhibition of MDA-7 results in transformation and progression from a local, nonmetastatic primary tumor to a highly metastatic phenotype. Additional studies have shown that Ad-mda7 can inhibit cell migration and invasion of lung and breast tumor cells by downregulating the PI3K pathway and inhibiting production of FAK and matrix metalloproteases [22,27]. Tumor cells expressing MDA-7 demonstrated significantly reduced lung metastases compared to control cells [27,32]. It is clear that tumor cells can develop resistance to cytotoxic therapies, and reports are now emerging of acquisition of resistance to pathway-specific molecularly targeted therapeutics. The anti-tumor effects mediated by MDA-7 encompass a variety of signaling pathways, and it is anticipated that redundant proapoptotic signals are activated.

In summary, INGN 241 can induce apoptosis in a large percentage of tumor volume following a single intratumoral injection; however, clinically significant responses are primarily seen with repeat injection. Future studies, therefore, will concentrate on repeat dosing of INGN 241, particularly in malignant melanoma, in which the greatest clinical activity was seen in this study. Other future directions include developing systemic administration of INGN 241, given its widespread tumor selectivity, exploration of its immunopotentiating effects, and its use in combinatorial strategies.

Patients and Methods

The clinical protocol used in this study was reviewed by the Biosafety Committee of each participating institution and the U.S. Food and Drug Administration. Written informed consent was obtained from all patients stating that they were aware of the investigational nature of this study, in keeping with institutional and federal guidelines. For inclusion in this study, patients had to be at least 18 years of age with histologically confirmed carcinoma and at least one lesion accessible for needle injection. A Karnofsky performance status of ≥70% was required as was acceptable hematologic, renal, and hepatic function. No patient with active CNS metastases, chronic immunosuppressive use, or prior participation in a therapy requiring the administration of adenovirus was allowed.

Description of agent

INGN 241 is constructed from an adenoviral vector deleted in the E1 and a small portion of the E3 regions to render it replication defective. The vector contains a transgene region encoding a wild-type human *mda-7* cDNA driven by the cytomegalovirus immediate early promoter and ending in an SV40 polyadenylation signal and has been described previously [5]. INGN 241 was provided as a frozen vial suspension (3.0-ml vial) at a concentration of 1×10^{12} vp/ml (5×10^{10} PFU/ml) in a neutral buffer containing saline and 10% glycerol. The vials were stored at ≤60°C. Prior to injection, vials were thawed to ambient temperature and then mixed with 5% glucose solution to obtain the appropriate number of viral particles in a total volume of 2.0 ml. To aid in localization of the injection site, 0.4 ml of Isosulfan blue dye was added just prior to injection. Previous studies demonstrated that Isosulfan blue did not negatively impact vector transduction (unpublished data).

Study design

Patients were treated in the outpatient research centers of the Mary Crowley Medical Research Center at Baylor University Medical Center (Dallas, TX, USA) or the Tyler Cancer Center (Tyler, TX, USA). All patients signed the U.S. Oncology Institutional Review Board approved consent form prior to entry on the trial.

Patients were initially enrolled in sequential cohorts receiving doses of the INGN 241 construct escalating

doi:10.1016/j.ymthe.2004.09.019

from 2×10^{10} to 2×10^{12} vp (see Table 1 and Fig. 1). The injections were placed in the center of the accessible target tumor lesion. In the first three cohorts (encompassing the dose range 2×10^{10} to 2×10^{12} viral particles), the injected lesion was resected 24 h after injection. The next two patient cohorts continued to receive 2×10^{12} vp without escalation, but with tumor resection at either 48 (cohort 4) or 96 h (cohort 5) postinjection. The resected lesions were bisected (see schematic in Fig. 2): one hemilesion was serially sectioned, fixed in paraformaldehyde, and paraffin embedded (for immunohistochemical evaluation) and the other hemilesion was serially sectioned and immediately frozen in liquid nitrogen (for quantitative nucleic acid evaluation). Samples were analyzed to determine the radius of diffusion of injection solution, the distribution and concentration of the viral agent, mRNA and protein expression, and the resultant biologic effects on the tumor cells (Fig. 2). Blood was also sampled for vector DNA. A single patient cohort (cohort 6) received a total dose of 2×10^{12} vp divided into 10 deposit sites with injections of 0.2 ml at each site, with subsequent resection of the lesion 48 h postinjection.

To assess longer term effects of MDA-7 expression, as well as the effects of repeat injections, the final two cohorts did not undergo excision but instead had incisional biopsies performed pretreatment and 30 days posttreatment. In one cohort (cohort 7), a single injection was carried out on day 1 and then an incisional biopsy was performed 30 days later. In the other cohort (cohort 8), 2×10^{12} vp were injected twice weekly for 3 weeks of a 28-day cycle, with a maximum of two cycles permitted. Tumor responses were measured at the end of each cycle and an incisional biopsy was carried out 30 days after the last injection. Tumor responses were evaluated using the RECIST methodology for each indicator lesion. All patients were monitored throughout for development of toxicity related to either the agent or the injection. The full treatment schema is outlined in Fig. 1.

Laboratory analyses

From the biopsy specimens, frozen tissue was obtained for quantitative DNA PCR for INGN 241 DNA and for RT-PCR for *mda-7* mRNA. Paraffin sections of biopsy specimens were analyzed for morphology, immunohistochemistry staining for the MDA-7 protein, and TUNEL analysis of the percentage of apoptotic cells. A previously described automated immunoperoxidase staining technique [14] was used to characterize protein expression following antigen retrieval, with the use of the Ventana 320 ES System (Ventana Medical Systems, Tucson, AZ, USA) and the avidin–biotin-complexed immunoperoxidase reaction (DAB detection kit; Ventana Medical Systems) following initial incubation with affinity-purified rabbit anti-human MDA-7 antibody (Introgen Therapeutics). A TUNEL method (DeadEnd Colorimetric Apoptosis Detection System; Promega) was used to detect DNA fragmentation *in situ*. The frequency of MDA-positive or TUNEL-positive cells was determined as an averaged value of the proportion of positive-cells in three 100× power microscopic fields of representative staining pattern. Tumor cell types were distinguished from normal cells and/or infiltrating lymphoid cells by histological criteria by a trained histopathologist.

To characterize systemic immune activation, ELISAs (R&D Quantikine kits; Minneapolis, MN, USA) were used to quantify patient serum cytokine levels at defined time points before and after treatment [15]. In addition, flow cytometric immunophenotype analysis was carried with a two-color immunofluorescence reaction to determine the effect of INGN 241 on peripheral blood frequency distribution of T, B, and NK subsets [16]. More extensive descriptions of these studies are provided in another article [31].

RECEIVED FOR PUBLICATION MAY 18, 2004; ACCEPTED SEPTEMBER 28, 2004.

REFERENCES

1. Jiang, H., *et al.* (1995). Subtraction hybridization identifies a novel melanoma differentiation associated gene, mda-7, modulated during human melanoma differentiation, growth and progression. *Oncogene* **11:** 2477–2486.
2. Kotenko, S. V. (2002). The family of IL-10-related cytokines and their receptors: related, but to what extent? *Cytokine Growth Factor Rev.* **13:** 223–240.
3. Chada, S., *et al.* (2004). MDA-7/IL-24 is a unique cytokine in the IL-10 family. *Int. Immunopharmacol.* **4:** 649–667.
4. Caudell, E. G., *et al.* (2002). The protein product of the tumor suppressor gene, melanoma differentiation-associated gene 7, exhibits immunostimulatory activity and is designated IL-24. *J. Immunol.* **168:** 6041–6046.
5. Mhashilkar, A. M., *et al.* (2001). Melanoma differentiation associated gene-7 (mda-7): a novel anti-tumor gene for cancer gene therapy. *Mol. Med.* **7:** 271–282.
6. Ekmekcioglu, S., *et al.* (2001). Down-regulated melanoma differentiation associated gene (mda-7) expression in human melanomas. *Int. J. Cancer* **94:** 54–59.
7. Saeki, T., *et al.* (2001). Tumor-suppressive effects by adenovirus-mediated mda-7 gene transfer in non-small cell lung cancer cell in vitro. *Gene Ther.* **7:** 2051–2057.
8. Jiang, H., *et al.* (1996). The melanoma differentiation associated gene mda-7 suppresses cancer cell growth. *Proc. Natl. Acad. Sci. USA* **93:** 9160–9165.
9. Su, Z. Z., *et al.* (1998). The cancer growth suppressor gene mda-7 selectively induces apoptosis in human breast cancer cells and inhibits tumor growth in nude mice. *Proc. Natl. Acad. Sci. USA* **95:** 14400–14405.
10. Saeki, T., *et al.* (2002). Inhibition of human lung cancer growth following adenovirus-mediated mda-7 gene expression in vivo. *Oncogene* **21:** 4558–4566.
11. Fisher, P. B., *et al.* (2003). mda-7/IL-24, a novel cancer selective apoptosis inducing cytokine gene: from the laboratory into the clinic. *Cancer Biol. Ther.* **2**(4 Suppl. 1): S23–S37.
12. Nishikawa, T., Ramesh, R., Chada, S., and Meyn, R. E. (2004). Suppression of tumor growth and angiogenesis by adenovirus-mediated mda-7/IL-24 gene transfer in combination with ionizing radiation. *Mol. Ther.* **9:** 818–828.
13. McKenzie, T., Liu, Y., Fanale, M., Swisher, S. G., Chada, S., and Hunt, K. K. (2004). Combination therapy of Ad-mda7 and trastuzumab increases cell death in Her-2/Neu-overexpressing breast cancer cells. *Surgery* **136:** 437–442.
14. Nemunaitis, J., *et al.* (1998). Prognostic value of K-ras mutations, ras oncoprotein, and c-erb B-2 oncoprotein expression in adenocarcinoma of the lung. *Am. J. Clin. Oncol.* **21:** 155–160.
15. Nemunaitis, J., *et al.* (2001). Intravenous infusion of a replication-selective adenovirus (ONYX-015) in cancer patients: safety, feasibility and biological activity. *Gene Ther.* **8:** 746–759.
16. Zhang, X., Qian, J., and Li, J. (2000). [Clinical and experimental analysis of myeloid antigen positive childhood acute lymphoblastic leukemia]. *Zhongguo Shi Yan Xue Ye Xue Za Zhi* **8:** 280–282.
17. Sieger, K. A., *et al.* (2004). The tumor suppressor activity of MDA-7/IL-24 is mediated by intracellular protein expression in NSCLC cells. *Mol. Ther.* **9:** 355–367.
18. Ramesh, R., *et al.* (2003). Melanoma differentiation-associated gene 7/interleukin (IL)-

24 is a novel ligand that regulates angiogenesis via the IL-22 receptor. *Cancer Res.* **63:** 5105–5113.
19. Swisher, S. G., *et al.* (1999). Adenovirus-mediated p53 gene transfer in advanced non-small-cell lung cancer. *J. Natl. Cancer Inst.* **91:** 763–771.
20. Lang, F. F., *et al.* (2003). Phase I trial of adenovirus-mediated p53 gene therapy for recurrent glioma: biological and clinical results. *J. Clin. Oncol.* **21:** 2508–2518.
21. Ellerhorst, J. A., *et al.* (2002). Loss of MDA-7 expression with progression of melanoma. *J. Clin. Oncol.* **20:** 1069–1074.
22. Mhashilkar, A. M., *et al.* (2003). MDA-7 negatively regulates the β-catenin and PI3K signaling pathways in breast and lung tumor cells. *Mol. Ther.* **8:** 207–219.
23. Pataer, A., *et al.* (2002). mda-7 induces apoptosis via upregulation of the double-stranded RNA dependent kinase PKR. *Cancer Res.* **62:** 2239–2243.
24. Pataer, A., Chada, S., Hunt, K. K., Roth, J. A., and Swisher, S. G. (2003). Adenoviral MDA-7 induces apoptosis in lung cancer cells through mitochondrial permeability transition independent cytochrome c release. *J. Thoracic Cardiovasc. Surg.* **126:** 1325–1328.
25. Cao, X. X., *et al.* (2002). Adenoviral transfer of mda-7 leads to BAX up-regulation and apoptosis in mesothelioma cells, and is abrogated by over-expression of BCL-XL. *Mol. Med.* **8:** 869–876.
26. Ekmekcioglu, S., *et al.* (2003). Negative association of melanoma differentiation associated gene (mda-7) and inducible nitric oxide synthase (iNOS) in human melanoma: MDA-7 regulates iNOS expression in melanoma cells. *Mol. Cancer Ther.* **2:** 9–17.
27. Ramesh, R., Ito, I., Gopalan, B., Saito, Y., Mhashilkar, A. M., and Chada, S. (2004). Ectopic production of MDA-7/IL-24 inhibits invasion and migration of human lung cancer cells. *Mol. Ther.* **9:** 510–518.
28. Kawabe, S., Nishikawa, T., Munshi, A., Roth, J. A., Chada, S., and Meyn, R. (2002). Adenovirus mediated mda-7 gene expression radiosensitizes non-small lung cancer cells via p53-independent mechanisms. *Mol. Ther.* **6:** 637–644.
29. Chada, S., Ramesh, R., and Mhashilkar, A. M. (2003). Cytokine- and chemokine-based gene therapy for cancer. *Curr. Opin. Mol. Ther.* **5:** 463–474.
30. Chada, S., *et al.* (2004). Bystander activity of Ad-mda7: human MDA-7 protein kills melanoma cells via an IL-20 receptor-dependent but STAT3-independent mechanism. *Mol. Ther.* (in press).
31. Tong, A., *et al.* (2004). Intratumoral injection of INGN 241, a non-replicating adenovector expressing the melanoma-differentiation associated antigen-7 (MDA-7/IL-24): biologic outcome in advanced cancer patients. *Mol. Ther.*, (in press).
32. Ramesh, *et al.* (2004). Liposome-mediated *mda7/IL-24* gene delivery inhibits human lung cancer growth in *in vivo*. *DNA Cell Biol.*, (in press).